Instytut Agrofizyki
im. Bohdana Dobrzańskiego PAN
w Lublinie

ACTA AGROPHYSICA

25

Stefan Szwaj, Adam Pukos

PLOWING THEORY

Monografia

Lublin 2000

Adres redakcji

Instytut Agrofizyki im. Bohdana Dobrzańskiego PAN
ul. Doświadczalna 4, P.O. Box 201, 20-290 Lublin 27
tel. (0-81) 744-50-61, e-mail: fundacja@demeter.ipan.lublin.pl

Publikacja indeksowana przez
Polish Scientific Journals Contents - Agric. & Biol. Sci.
w sieci Internet pod adresem http://saturn.ci.uw.edu.pl/psjc/
lub http://ciuw.warman.net.pl/alf/psjc

Pracę częściowo wykonano w ramach projektu badawczego Nr 5 P06F005 08
finansowanego przez Komitet Badań Naukowych

ISBN 83-87385-37-9
ISSN 1234-4125

Wydanie I. Nakład 150 egz. Ark. wyd. 4,4
Skład komputerowy: doc. dr hab. Adam Pukos
Druk: Zakład Usług Poligraficznych TEKST s.c., ul. Wspólna 19, 20-344 Lublin

CONTENTS

PREFACE

The plowing problem is well elaborated from the practical side, but not theoretically satisfactory. Only some authors have studied this problem theoretically [2,11,12,14,32, 48] but indeed they have not exposed the soil parameters, which influence the process very much. Similar situation exists in the metal processing, where the main attention is paid to the geometrical shape and the quality of surface [21].

The topic problem in the present paper is to consider globally many agents influencing the plowing process using heuristic method [37]. The following features are taken into consideration first off all: soil parameters, implement form, plowing speed and the process of clod forming. On that base the moldboard surface is mathematically described and next a trajectory of soil particles motion formulated, then the speed and accelerations are calculated. These allow to calculate the forces acting on the plow moldboard, exerted by clod, and also the forces acting on a shear blade, upon an edge of landside of the moldboard and on the landside separating surface forming the vertical plane. These details are discussed later, but beneath some assumptions concerning the problem are presented.

ASSUMPTIONS

The method applied treats the plowing problem in a complete way considering the soil proportions, implement form, dynamic factors and a mechanism of the process altogether. The trajectory of soil particles, then the speed, acceleration and forces acting at different parts of plow bottom are calculated. For that reason many Figures are presented in prospective views, preserving some notation and coordinates systems. These coordinates are as presented in Fig.1a and shown later in other Figures. They are as follows: Cartesian coordinates combined with the field $\overline{O}_a\overline{y}_1\overline{y}_2\overline{y}_3$, $O_B u_1 u_2 u_3$, $O_{\bar{c}} y_1 y_2 y_3$, cylindrical coordinates combined with the moldboard $O_F r \vartheta z$, Cartesian coordinates which are combined directly with the moving moldboard $O_a y_1' y_2' y_3'$, $Oz_1 z_2 z_3$, $O_L w_1' w_2' w_3'$, $O_F x_1' x_2' x_3'$, and any natural coordinate system combined with a chosen point of trajectory line. Between them there exist all the defined transformations, allowing transferring certain values from one system to another. Also some assumption are separately introduced for the soil and other features of the subject being studied.

The soil alone is considered as a homogenous, isotropic, physically nonlinear compressible medium, changing its parameters depending on moisture, stress as well as strain values in conventional sense, contradictory to the logarithmic ones [16]. Under some load it arrives at a limit state, defined by yield criteria, typical for certain material [15,25].

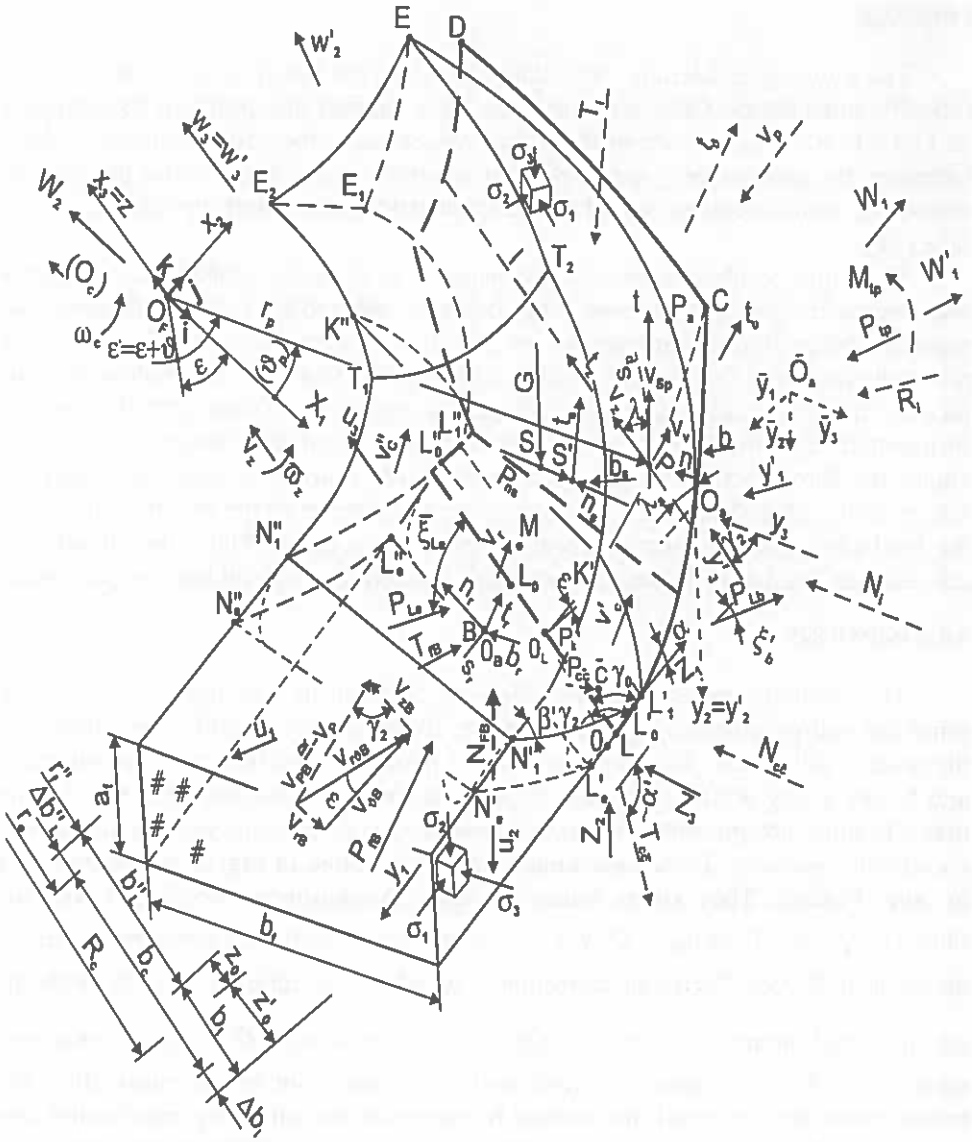

Fig.1a. Scheme of plowing.

It should be mentioned here, that in some new papers [28,29] the soil was treated in another way, describing the deformation process as the motion of soil particles and aggregates into empty pores, which are large enough for them to enter.

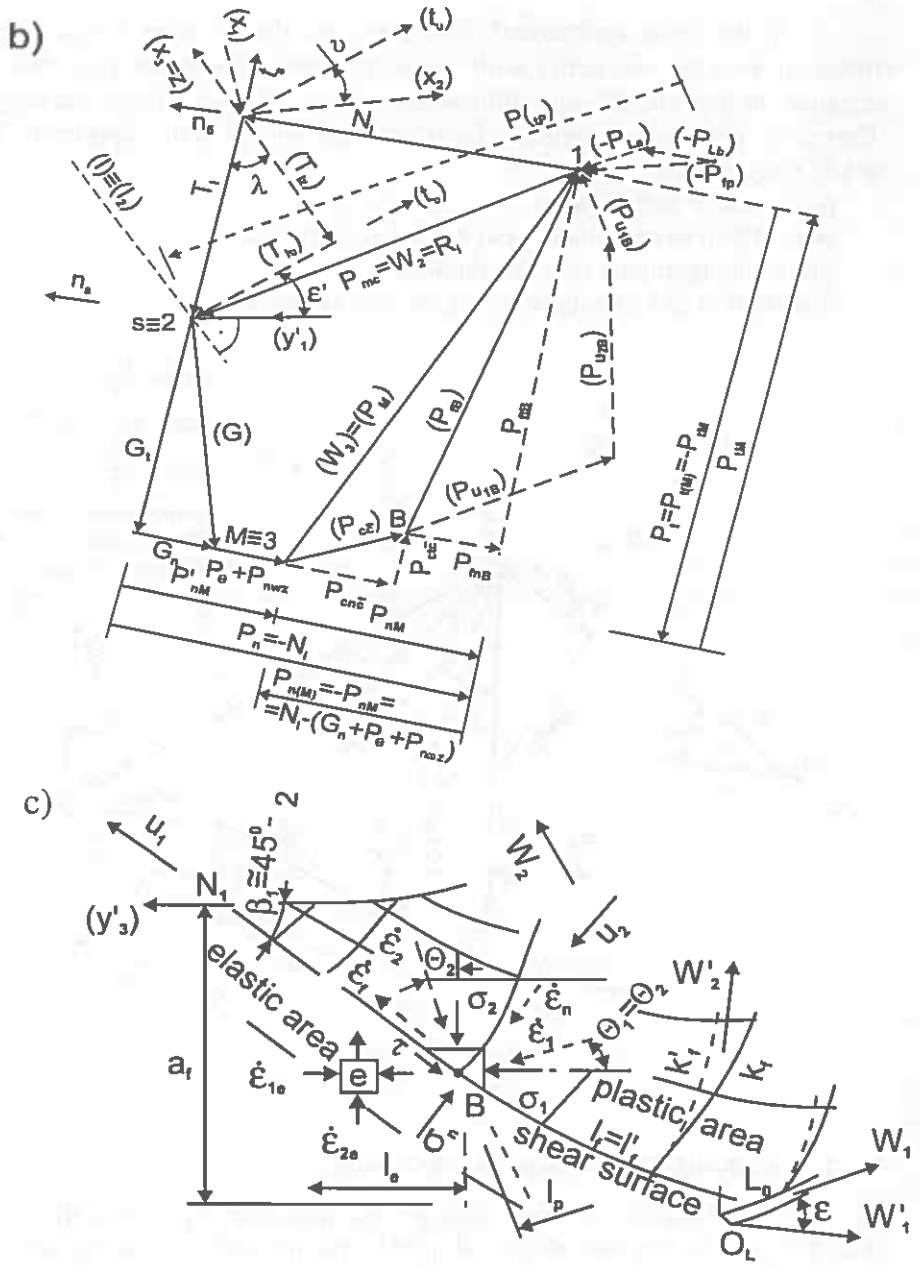

Fig. 1. (Cont.) b – projection of forces, c – kinematics of clod deformation.

In the loose agricultural soils there are always some larger free spaces filled up with air and partly with water (40÷70% of soil volume). Such action depends on the strength and dimensions of soil pores, particles and aggregates. Therefore four random variables have been introduced in this approach. The values of these variables are:

- pore volume distribution,
- pore effective maximum cross section distribution,
- grain and aggregate size distribution,
- distribution of forces between grains and aggregates.

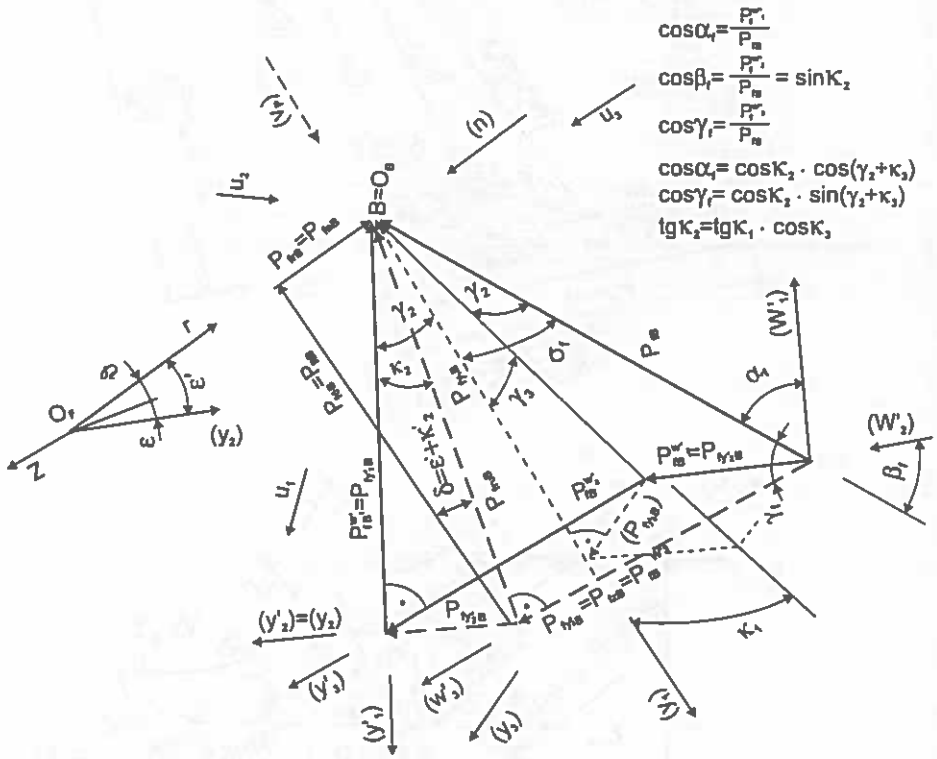

Fig. 1. (cont.) **d** – scheme of forces acting in front surface.

They are distribution function (histograms) obtained experimentally and introduced for the description of the soil initial structure and its changes during deformation. The method appeared especially effective in prediction of the evolution of the pore size distribution during soil deformation and will be presented in next paper about dynamic and volume effects of plowing.

Under a load, before the limit state appears, the soil has two types of deformations (elastic and plastic) as well as viscous flow, dependent on the rate of process. Its deformation rule suits Kelvin's rheological model adapted to big volume changes. The following formula describes the relation between stress and strain tensors [36,37,40]:

$$S = S' + S'' = 2GT' + 3KT'' + 2\lambda\dot{T}' + 3\kappa\dot{T}'', \qquad (1)$$

where S' denotes stress deviator, S''- isotropic part of stress tensor G, K – rigidity and bulk modulus; λ, κ - coefficient of resistance dependent on nondilattional (λ) and dilatational (κ) strains, T' - strain deviator, T'' - isotropic component of total strain tensor and $\dot{T}$ strain velocity tensor for a certain part.

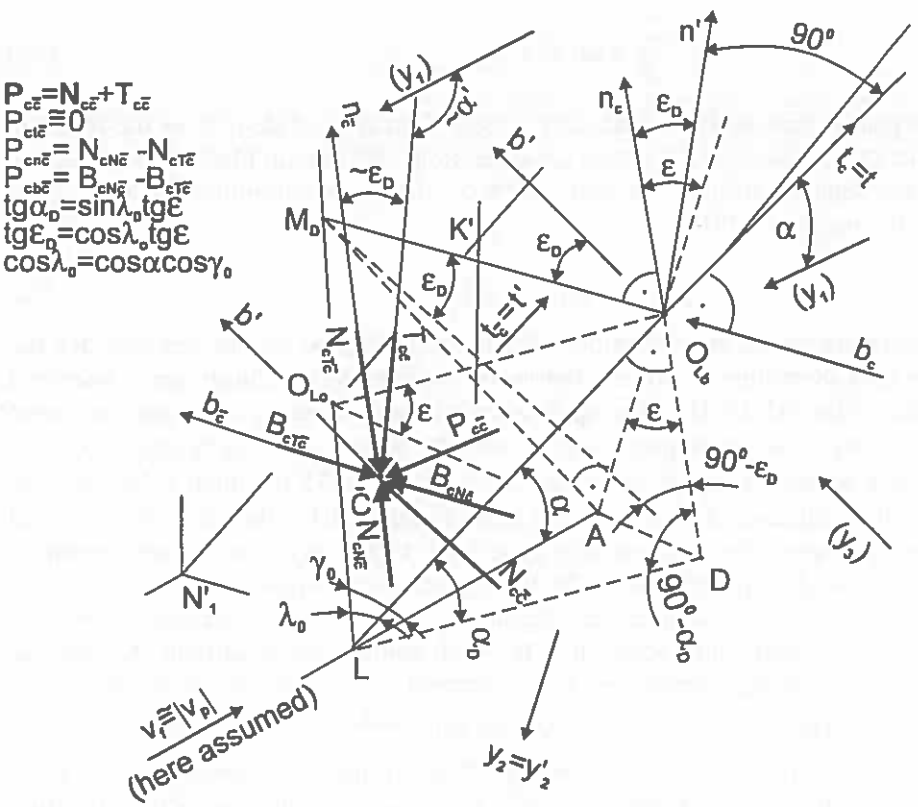

Fig. 1. (Cont.) e – scheme of forces acting in landside separation surface.

Such medium fulfils a motion equation:

$$\rho(\vec{a}-\vec{F}) = \text{Div}\, S, \tag{2}$$

where: ρ is soil density, $\vec{a}$ - acceleration of particle, $\vec{F}$ - mass force, Div S - divergence of stress tensor; the capital D denotes its vector character, to distinguish it from divergence of vector being a scalar. That equation can be transferred to another form, written in a vector notation:

$$(K+\frac{G}{3})\,\text{grad}\,\text{div}\,\vec{u}\;G\nabla^2\vec{u}+(\kappa+\frac{\lambda}{3})\text{grad}\,\text{div}\,\vec{\upsilon}+\lambda\nabla^2\vec{\upsilon}=\rho(\vec{a}-\vec{F}), \tag{2a}$$

where ∇^2 - Laplacian, $\vec{u}$ -displacement vector, $\vec{\upsilon}$ - velocity vector. Additionally that soil fulfils the equation of continuity:

$$\frac{\partial\rho}{\partial t}+\text{div}\,\vec{\upsilon}=0, \tag{2b}$$

where partial time derivative denotes a local derivative of density as the function of time. On the basis of the above considerations, for certain places where density does not depend on time, but only on place, the soil's continuity equation takes the following form [39]:

$$\vec{\upsilon}\,\text{grad}\rho+\rho\,\text{div}\,\vec{\upsilon}=0. \tag{2c}$$

The thermodynamic and filtration process are not being considered here for the reason of a short time of process before the soil reaches the limit state, described by other rules [15,17,31]. The application of those rules to study the action of tools, having a flat work path, is given in [39], where the motion equation (2) is simplified assuming $\vec{a}=0$ at a low tool's speed 1÷1.15 m/s then it becomes an equilibrium equation. Decomposition of that equation for the parts gives partial differential equations of hyperbolic type [47], to be solved at certain boundary and initial condition limitations. The tool action itself evokes some limit states in subsoil with some slip surfaces accompanying them, adequate to characteristics of tension's field, defined by solution of the limit equilibrium equations. It happened when the soil strength drawn out at the moment of equality of two main stresses (e.g. $\sigma_2 = \sigma_3$) presenting a case of any total limit states of stresses [31, 39].

Additionally the angle between directions of the main stresses and the main strain rates should be defined by solving the deviation equation, which, together with continuity equation, defines certain field of the translation of soil mass, defining solution admissibility from the kinematics point of view. That procedure is

quite complicate therefore, for simplicity sake, it is assumed that the main mean stress (σ_3 parallel to the axis y_3) coincides with the main mean rate of deformation ($\dot{\varepsilon}_3$). Then the angle between them equals $\theta_3 = 0$.

If additionally an adequate angle θ_1 between σ_1 and $\dot{\varepsilon}_1$ as well as σ_2 and $\dot{\varepsilon}_2$ is equaled to $1/2\phi_f$ then the shear surfaces (being characteristics of the stress field) coincide with the characteristics of the strain rate field. In such a case the maximum rate of tangential strains coincides with the slip surfaces (lines) [17], which is schematically shown in Fig.1c. This fact is accounted for in our analysis.

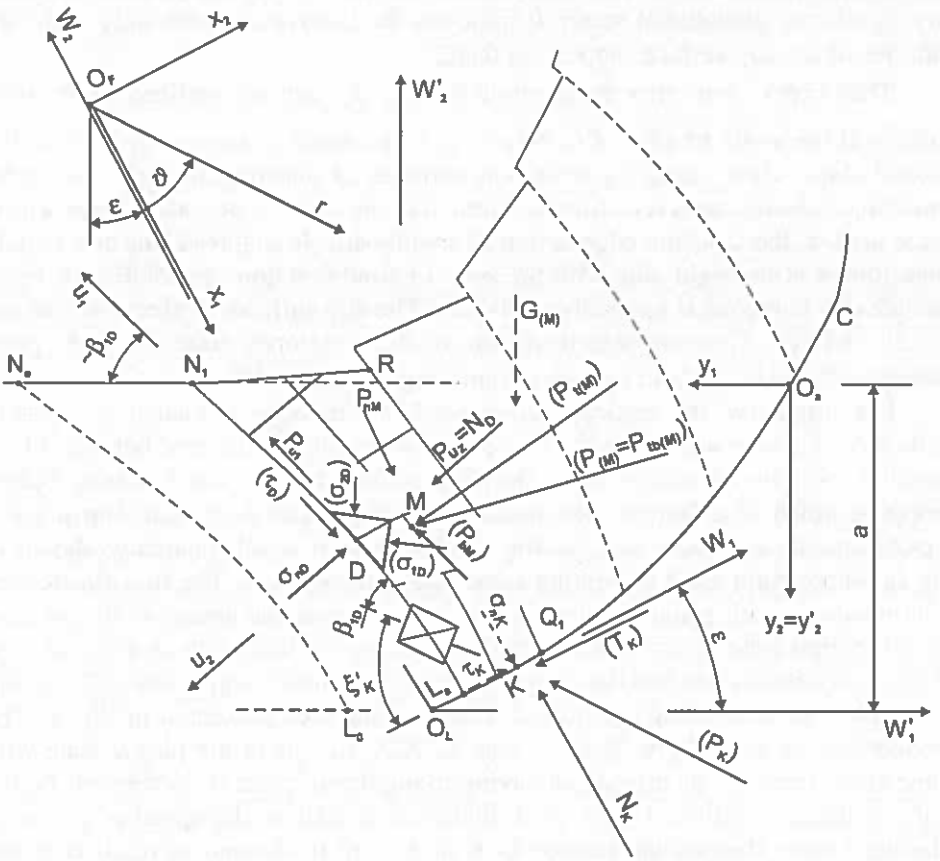

Fig.1. (Cont.) f – scheme of forces for 2nd type of clod forming.

The soil being analyzed possesses also some cohesion and adhesion to steel some value of internal friction and external friction against steel. These soil parameters depend on components, moisture, density and the speed of deformation [36,37].

The soil plowed can be separated from the ground in two main ways: by compression of loose subsoil mass (Fig. 1a) and by tearing off each clod's part piece by piece from a dense soil base (Fig. 1f). In the first case the soil can be in elastic or plastic, active or passive state [42], different in form and depending on the place. The elastic state is characterized by some dilatational together with nondilatational strains [37] existing in a certain area (e.g. lines $L_e'N_e'N_e''L_e''$ and $L_0'N_1'N_1''L_0''$). The area of the elastic state exists in the area mentioned above and in the rear part of moldboard (behind the line $L_1'K'K''L_1''$). The plastic state, creating the passive limit state above the share (L_0' N_1' $N_1''L_0''$), does not show any significant dilatational strain. It indicates the transverse strain only with two families of the slip surfaces appearing there.

They cross each other at the angle of $90^0 - \phi_f$ and are inclined to the field surface at the angle of $45^0 - \phi_f/2$, where ϕ_f is the angle of internal friction in the natural state. They create some frontal surfaces of shearing in field soil to be sometimes clearly observed. Another limit state of active type, takes place within some area of the landside edge action of moldboard. It is spread out in a certain zone joined at the right side with the zone of frontal action of moldboard. From the left side that zone is gradually vanishing. The slip surfaces of that zone are not exactly defined. They are placed in front of the mentioned edge along the plow motion inclined to the land surface at same angle equal to $45^0+\phi_f/2$.

For simplicity, the vertical plane traced by side edge is treated as a potentially side shearing surface. In the rear part of a moldboard the clod behaves like a granular medium in elastic state, showing some cracking and breaking before dropping down to a furrow. The process and the forces accompanying it for a typical agricultural loose soil, having small cohesion is schematically shown in Fig.1a with certain areas presenting some states in soil mass. The first elastic area is a transit one with gradual increase of the tension from the natural field soil state up to the limit state. It can be estimated running triaxial tests with an adequate soil at the compression rate and the sample volume decrement, registered [37], similar to the plow process being considered, based on the idea presented in Fig. 6. The second area between $L_0'N_1'N_1''L_1''$ and $L_1'K'K''L_1''$ is in the plastic state with some shear surfaces. Its dimension having triangular-trapesic form depends on the soil condition, moldboard type, clod thickness as well as the speed of plowing. The third area (behind the surface $L_1'K'K''L_1''$ up to the end of clod) is in the elastic state where the stresses are getting smaller for the sake of reduction of clod moving resistance. At the end, the soil (of a granular type) is going to drop or slip down over the surface forming certain slope $ET_2T_1E_2$, dependent on the soil condition and the plowing process. That slope can be defined with a simplified Senkov's formula [15]. The shear edge locally produces the limit state in the field

soil, which is discussed later. A similar action takes place on the landside edge of the moldboard.

The stresses distributions in some areas as well as on the surfaces are not defined, therefore these data are further replaced by adequate forces, acting in certain points representing the centers of gravity of chosen parts of clod or surfaces. These forces are transmitted from one place to another through the soil mass, respecting adequate direction. A basic mechanism of clod separation from the field of the first type for a granular soil (neglecting local cutting edges action) goes that way that the part of soil above the share is lifted up. Then it is sliding over the moldboard and also over the frontal sharing surface $L_0'N_1'\ N_1''L_0''$ along the side shearing surface $L_1'L_0'\ N_1'K'$ (Fig. 1a). The clod thickness still increases its value, sufficient to transmit some forces in the range sufficient to overcome the soil shearing resistance on the frontal and the side shearing surfaces. In the case of heavy dense soil (dry clay) the separation mechanism goes by tearing off piece by piece clod parts from the field.

The plow moves with a constant horizontal speed υ_p but the soil in clod decreases its speed versus implement because of clod deformation. During that time the clod is double bent and additionally twisted. For the first time it is bent around the z-axis. For the second time it is bent around temporary rotation axis, located to the right of the plow bottom. It takes place due to the different deformation rates existing between the left and right side of clod. After that the clod is twisted, turned and thrown side-ways to the furrow. The forces accompanying that process are being studied independent of the forces on cutting edges. The orientation of some forces acting upon the chosen clod element moving along the trajectory depends on the position of that element on this trajectory, characterized by unit vectors (tangent - t, normal - n, and binormal - b [7,18,30].

This creates the dynamic problem to be solved after formulation the moldboard equation in a cylindrical system of axes $(r\vartheta\varphi)$. But beneath, on a base of Fig. 1b, the forces acting upon the plow are presented in a global view projected onto the plane traced by the unit vectors t and n and crossing the center of clod gravity. Real lengths of force vectors are given without brackets, but their projections in brackets. Certain point axes and angles characterizing the problem are also marked there.

The forces are as follow: P_{le} is the horizontal subsoil reaction against subsoil penetration by the share edge inclined at some angle ξ_l to that edge, P_{lb} - soil reaction against local soil penetration by the moldboard's side edge. It is inclined at the angle ξ'_b to the plow motion, P_{fp} is the resultant force of two previous ones, $P_{c\tau}$ - soil reaction against the clod separation from the field along the landside surface of furrow located in its middle point $\overline{C}$. It is first decomposed into two

components: $N_{c\bar{c}}$ and $T_{c\bar{c}}$, inclined at an angle α' to the field level (Fig. 1e), next transformed to the natural system related to the trajectory line going through the point $\overline{C}$, P_{fB} represents field action against the clod separation in front of the share. It acts in the point B and is inclined at some angles κ_1, κ_2, κ_3 in reference to the y_1 axis (Fig. 1d). It is then decomposed into next following three components: P_{frB} - parallel to the unit vector n, $P_{f\vartheta B}$ - parallel to the direction t_ϑ, and P_{fzB} - parallel to the z-axis. G represents the clod weight charging the plow body and both separation surfaces consisting of tangent component G_t, normal G_n (Fig. 1b) and binormal G_b (not shown). $P_{n\omega_z}$ is the centrifugal force provoked by clod rotation around the z-axis, continuously changing, and P_θ - normal force evoked by the effect of pushing the clod over the curved implement. The sum of components:

$$P_{fnB} + P_{cn\bar{c}} + G_n + P_{n\omega_z} + P_\theta = P_n \tag{3}$$

gives an entire normal force exerted by the clod upon the implement. It provokes, due to the soil metal friction and adhesion, some moving resistance T_t against the clod motion (Fig. 1b). This resistance together with the normal force P_n taken with opposite sign gives a resultant moldboard action R_i against the clod. It equals to the geometrical sum of previously mentioned forces

$$\vec{R}_i = \vec{P}_{mc} = \vec{P}_{fb} + \vec{P}_{c\bar{c}} + \vec{G} + \vec{P}_{n\omega_z} + \vec{P}_\theta . \tag{3a}$$

Adding geometrically the action of two implement edges (P_{le}, P_{lb}) to that sum one gets the total plow action against the soil being plowed. The resultant force P_{lp} (Fig.1a) is located in space with some inclination to the axes of a chosen system of coordinates. That resultant defines a reduction line (central axis) of spherical forces in relation to which the sum of moments M_{lp} of the forces mentioned is constant [20]. These values can be calculated providing the forces and theirs directions are known or found out by means of tests run on special equipment [9]. These data and the assumption presented (concerning the plowing process) belong to its main energetic problems. However we do not include any micropolar elastokinetics problems involving the Cosserat brothers' theory [23] to be presumably helpful for more precise investigation.

MOLDBOARD EQUATION

Directrix and generating lines (Fig.2.) define the moldboard here. This equation is given in a cylindrical coordinates system $O_F r \vartheta z$, Fig. 3. It is for simplicity

assumed that a directive curve of the moldboard surface makes a segment of an ellipse, defined by the equation defining the radius of that curve:

$$r(\vartheta) = \frac{p}{1 + e\cos\vartheta}, \tag{4}$$

where $p = \frac{b^2}{a}$ is a parameter, $e = \frac{c}{a}$ (1 denotes eccentricity, a and b – bigger and smaller ellipse axis, c - focal ellipse length.

That curve is constructed in such a way that it goes through three points O_L, B, C (Figs 2a, 2b) adequately chosen for the implement designed. This formula adopted from the ballistic technology [1] can be written in a form:

$$p = \frac{r_{ol} r_B [\sin(45^\circ - \varepsilon/2) + \cos\varepsilon]}{r_B \sin(45^0 - \varepsilon/2) + r_{ol}\cos\varepsilon}, \tag{5}$$

where: ε is the angle shown in Figs 1, 2a and $r_{O_L} = r_c = R$, $r_B = R + \Delta R$, $\varepsilon = \frac{p - R}{R}$. It is also possible to use another curve for the directrix line e.g. a segment of the circle (ε = 0, $p \neq 0$), parabola (ε = 1) or hyperbola (ε 〉1), (or vertical straight line for p = 0). The generating lines go through the chosen directrix (k) at different angles $\bar{\gamma}$ corresponding to the γ angles (Fig 2c). An alternation of the γ angles from the basic one $\gamma_2 = \gamma_{min}$ depends on the type of moldboard. Here the following formula is used [41]:

$$\Delta\bar{\gamma} = \gamma - \gamma_{\min} = \Delta\gamma(\vartheta) = k_\upsilon[1 - \cos(\vartheta - \vartheta_2)], \tag{5a}$$

where the coefficient k_υ is expressed by:

$$k_\upsilon = \frac{\gamma - \gamma_{\min}}{1 - \cos(\vartheta - \vartheta_2)} \tag{5b}$$

The value of the chosen angle γ (in radians) corresponds to the ϑ angle, but here ϑ_2 stands for γ_{min} (Fig 4). The coefficient k_υ has an undefined value for $\vartheta = \vartheta_2$. That problem can be considered near the ϑ_2 value, but then $\Delta\bar{\gamma} \cong 0$, therefore this fragment should be excluded from consideration. For the moldboard of a cylindrical type $k_\upsilon = 0$.

Using above relations, considering Fig. 3 and putting: $r_3' = r + \Delta r_3'$ one can write the moldboard equation in a form:

$$r_m(\vartheta z) = \frac{p}{1+e\cos\upsilon} - zk_\upsilon[1-\cos(\vartheta-\vartheta_2)]\cdot\sin\{\vartheta+\frac{z}{p}k_\upsilon\times$$
$$\times(1+e\cos\vartheta)[1-\cos(\vartheta-\vartheta_2)]\} \tag{6}$$

For practical reason this equation can be simplified to the form:

$$r(\vartheta z) = \frac{p}{1+e\cos\vartheta} - zk_\upsilon[1-\cos(\vartheta-\vartheta_2)]\sin\vartheta \tag{6a}$$

In that form the moldboard equation is applied further in this study.

PLOW BOTTOM ACTION

That problem has already been described in previous chapters. Here only some hints are given clarifying the reasons for the simplifications introduced. Behind the first transit elastic area begins the plastic deformation area presenting the passive limit state [42], with the slip surfaces $L_0'N_1'N_1''L_0''$ (Fig.1a), creating two families of shear surfaces (lines), crossing one another at the angle of $90^0 - \phi_f$ where ϕ_f is the angle of soil internal friction. These surfaces of a convex shape, later replaced by planes are inclined against the upper clod surface at the angle:

$$\beta' \cong \beta = 45^o - \frac{\phi_f}{2} \tag{7}$$

which is measured in a plane traced by two main stresses; the biggest one (σ_1) and the smallest one (σ_2). The main stress σ_1 is parallel the to the upper surface (Fig. 1a). This stress depends on the resultant force R_i presenting the implement action against clod and it is spread out all over the implement's surface-clod contact. Next the force R_i is transferred through the clod to the frontal and the side shear surfaces. They induce certain stresses all over those surfaces adequate to the limit states evoked there, giving shearing resistance forces $P_{fB}, P_{c\bar{c}}$ (Fig.1b). Contrary on a small contact area of clod with the implement ($L_a'L_a''L_1''L_1'$, Fig. 1a) the soil behaves like to be in an active limit state, presenting the case of negative friction [42]. The soil charges there the implement with the inclination of highest main stress to that surface at an angle schematically shown in Fig.5:

$$\xi_a = \tfrac{1}{2}(\varphi - arc\sin\frac{\sin\varphi}{\sin\phi}) \tag{8}$$

where φ denotes the angle of soil metal friction whereas ϕ - the angle of clod's soil internal friction.

This problem is essential for particular soil (sand) cultivated by shallow plowing and it can be neglected in other cases. Sometimes the inclination angle ξ_a can have the opposite direction. It happens during the implements upwards lifting, than the soil has a tendency to slip down, like from a ladder's shovel [42]. It can also, but very seldom, happen that a part of soil mass being in the passive limit state, presses upon certain part of the steel surface with the biggest main stresses at the angle:

$$\xi_p = \frac{1}{2}(180^o - \varphi - arc\sin\frac{\sin\varphi}{\sin\phi}) \tag{9}$$

Such a situation may exist during deep dry sand plowing, giving the effect similar to that, seen during the action of a bulldozer's blade or loader's shovel [39]; neglecting the difference between implement inclination to the motion. The plastic area, discussed in second chapter, vanish behind the surface $L_l'L_l''K'K''$. Next there begins the elastic area and it exists up to the moment of dropping the clod to a furrow. This process is important from agricultural viewpoint and will be discussed later.

Many features concerning the plowing problem are not precisely known. For example we do not know the way of the decomposition of the resultant force R_l (acting on the implement) for certain parts. We also do not known the stress and strain distribution in soil mass subjected plow action nor the problem whether the main strains' rates $(\dot{\varepsilon}_1, \dot{\varepsilon}_2, \dot{\varepsilon}_3)$ are parallel to the main stresses $(\sigma_1, \sigma_2, \sigma_3)$, in all places of that action, which is important from the kinematics point of view [17]. The pattern of connection of two separation areas (i.e. the side shearing area with the front shear area) is also unknown. Similarly the local stress distribution for the cutting edges (share and landside edge) is not exactly known. We can only assume that in front of those edges some limit states are being produced, depending on soil condition, cutting edge dimensions and a medium depth of soil penetration. Those actions are treated independently of other plowing actions. To calculate this resistance a formula was adopted from [39,40] which for the case of the share edge (Fig. 7f) is:

$$P_{Le} \cong \frac{b_f}{\sin\gamma_o} f_e[2c_f \operatorname{ctg}(45^o - \frac{\phi_f}{2}) + \gamma_f a_f \operatorname{ctg}^2(45^o - \frac{\phi_f}{2})] \tag{10}$$

where: a_f, b_f, f_b, γ_0 are dimensions of the clod and share, $f_a \cong 0.5$ cm stands for the thickness of the blade, γ_0 is shown in Fig.4a, whereas c_f, ϕ_f, γ_f stand for the cohe-

sion, angle of internal friction and unit weight for the soil in natural state respectively. This force acts against the edge at the angle: $\xi_{Le} = \xi_b$ (eq. (9)). Another force acting on the landside edge (Fig. 7b) can be expressed by:

$$P_{Lb} \cong a_f f_b [2c_f \operatorname{ctg}(45^o - \frac{\phi_f}{2}) + \frac{1}{2}\gamma_f a_f \operatorname{ctg}^2(45^o - \frac{\phi_f}{2})] \tag{11}$$

where f_b denotes the estimated thickness of the landside edge (equal to about 0.5÷1cm). It acts approximately at the angle

$$\xi_b' \cong \xi_b - \alpha - \Delta\alpha \tag{11a}$$

related to the direction of implement movement, where ξ_b is defined by eq. (9) and $\Delta\alpha$ is an increment of the angle related to ½ a_f.

The resistance of clod separation appears also on the landside surface of the furrow (approximately on the surface $O_a L_0' N_1'$ (Fig. 7a), but they are small and mainly dependent on the soil cohesion c as well as the area of that surface f_c. The mechanism of appearance of this resistance is not precisely known. Probably the land side edge, having a wedge shape, lifts up the soil, than locally some so called active limit state [42] is produced there, schematically shown in Fig. 7d. This evokes, near the upper part of field soil especially cohesive and with plant roots, the appearance of the area of extension stresses (Fig. 7c), with existence of some compression stresses deeper in the soil. This was presented in the diagram in Fig. 7f together with adequate Mohr circles ($M_{CL_0'}$) for vertical plane CL_0' (Fig. 7c).

For a cohesionless soil the compression stress stretch along the whole plowing depth. Similar problem exists for the loader's shovel discussed in [39], but here it is much simplified. The landside clod separation evokes the extension stress distribution in cohesive soil in the vertical plane $L_0' O_a N_1'$ (Fig. 7a) to some depth [42,45], Fig. 7c:

$$y_2^0 = \frac{2c_f}{\gamma_f} \operatorname{tg}(45^0 + \frac{\phi_f}{2}) \tag{12}$$

and fulfils the stress relation valid for the active state:

$$\sigma_A = \sigma_3 = -2c_f \operatorname{tg}(45^0 - \frac{\phi_f}{2}) + \gamma_f y_2 \operatorname{tg}^2(54^0 - \frac{\phi_f}{2}) \tag{12a}$$

$$\sigma_2 = \gamma_f y_2, \tag{12b}$$

$$\sigma_1 \cong k_0 \sigma_2 . \tag{12c}$$

Here k_0 is a coefficient of so-called lateral soil pressure at rest which amounts 0.4 – 0.8, but for overconsolidated soil its value is bigger and equals 2.5 – 3 [26, 45]. Beneath the depth y_2^0 the area of soil compression starts. The active state exists between in region marked by the line $O_a L_o'$ (Fig. 7a) and the horizontal lines $O_b N_{F'}$, $O_b N_{F''}$ (Fig. 7b) inclined at the same angle $\delta' < \gamma_2$ to the right and left side of plow motion. In that area some slip surfaces often appear (horizontal lines in Fig. 7b) crossing the main stresses σ_1 and σ_2 (see enlarged element $\bar{c}$ at the angle of $45^0 - 1/2\phi_f$. This shearing process can take place in the soil element $\bar{c}$ (also in the subsoil) along the plane 1536 or 2143 or even along the surface 253, depending on the alternating values of σ_2 (eq. (12b)), σ_1 (eq. (12c)) and σ_3 (eq. (12a), see Fig. 7f). Accepting the vertical position of the landside separation surface, the normal stress σ_n and the tangential stress τ can be calculated for a certain point, (e.g. F in Fig. 7). Assuming that the half part of the total surface of the landside separation surface approximately equals:

$$f_c \cong \frac{1}{2}\frac{a_f^2}{\operatorname{tg}\beta'}, \quad \operatorname{tg}\beta' \cong \cos\gamma_2 \operatorname{tg}(45^0 - \frac{\phi_f}{2}), \tag{12d}$$

soil can well resist against separation with the average stress values expressed by the formulas:

$$\sigma_{nev} = \frac{1}{2}(\sigma_n^{a_f} + \sigma_n^{o}) = \frac{1}{4}\{\gamma_f a_f [1 - \cos(90^0 - \phi_f)] + \\ + [-4c_f \operatorname{tg}(45^0 - \frac{\phi_f}{2}) + \gamma_f a_f \operatorname{tg}^2(45^0 - \frac{\phi_f}{2})][1 + \cos(90^0 - \phi_f)]\} \tag{13}$$

$$\tau_{ev} = \frac{1}{2}(\tau^{a_f} + \tau^{0}) = \frac{1}{4}\{\gamma_f a_f + [4c_f \operatorname{tg}(45^0 - \frac{\phi_f}{2}) - \\ - \gamma_f a_f \operatorname{tg}^2(45^0 - \frac{\phi_f}{2})]\sin(90^0 - \phi_f)\} \tag{13a}$$

where the upper indexes refer to the values of σ_3 (eq. (12a) and σ_2 eq. (12b)) for depth values equal to $y_2 = 0$ and $y_2 = a_f$. Thus the average values of the normal and tangential components of the landside separation force attached in the point $\bar{c}$ are described by:

$$N_{ceu} = \sigma_{neu} f_c$$

$$T_{ceu} = \tau_{eu} f_c \qquad (14)$$

giving the resultant force P_{ceu}.

The tangent component acts in the opposite direction to the absolute motion velocity of clod's particles versus the field level at the angle (Fig. 7a):

$$\alpha' = arc\ \mathrm{tg}\frac{\upsilon_f \sin\alpha}{\upsilon_f \cos\alpha - \upsilon_L} - \alpha - \Delta\varepsilon, \qquad (14b)$$

where υ_L is the velocity vector described later (see Fig. 8, υ_L) and $\Delta\alpha$ is described by eq. (11). This component helps to pull up the clod as it was described in [47]. The normal component N_{ceu} can have a positive sign (pulling force) or a negative one (pushing force).

The biggest resistance forces against the separation of clod appear on the front separation surface $L_0'N_1'N_1''L_0''$ (Fig.1a) in the cross-section - line $L_0 D$ - (Fig. 7g). It practically covers all the main resistance of the clod motion taking place at the moldboard. In other words, it amounts to the geometrical difference between implement force R_i=P_{mc} and the rest of the forces accompanying the plowing press, which is schematically presented in Fig. 1b by the following vector:

$$\vec{P}_f = \vec{R}_i - (\vec{P}_\theta + \vec{P}_{nw_3} + \vec{G} + \vec{P}_c). \qquad (14c)$$

The action of two cutting edges P_{Le} and P_{Lb} is excluded here. This problem requires a separate treatment, together with the soil mass transport problem, which is connected with the moldboard shape and the rate of the process and it will be presented in the next chapters.

SOIL MASS DEFORMATIONS AND ITS BEHAVIOUR ON THE PLOW BOTTOM

The plow action evokes some effect of speed decrement of the soil mass entering the moldboard caused by soil deformation described using the continuity equation (3a) specially adapted, written in the $O_L w_1' w_2' w_3'$ coordinate system combined with the moldboard (Figs 1a, 2). The soil mass is at first submitted to compression in the elastic area (Fig. 1c), with increasing intensity dependent on the plow position versus subsoil.

In that area, equation (1) describing the relation of stress tensors in reference to the strain tensors as well as to their rates, should be defined by triaxial test [37,38] based on the idea presented in the Fig. 6. Some of the results of such tests respecting previous notations are quoted beneath and used for the discussion of

our problem. Considering the two-dimensional state of soil deformations when the displacement $u_3 = 0$ (in the w_3' direction) and $\upsilon = \dot{u}$, it is possible to transform the continuity equation (3a) into the form [37]:

$$\frac{\partial \dot{u}_1}{\partial w_1'} + \frac{\partial \dot{u}_2}{\partial w_2'} = \dot{\varepsilon}_1 + \dot{\varepsilon}_2 = -\frac{\dot{u}_1}{\rho_o}\left(\frac{\partial \rho_o}{\partial w_1'} + \frac{\partial \rho_o}{\partial \sigma_m}\frac{\partial \sigma_m}{\partial w_1'}\right) - \\ -\frac{\dot{u}_2}{\rho_o}\left(\frac{\partial \rho_o}{\partial w_2'} + \frac{\partial \rho_o}{\partial \sigma_m}\frac{\partial \sigma_m}{\partial w_1'}\right) = \dot{\varepsilon}_v \tag{15}$$

In this relation

$$\sigma_m = \frac{1}{3}(\sigma_1 + \sigma_2 + \sigma_3), \quad \frac{\partial \rho_o}{\partial \sigma_m} = \kappa_o \tag{15a}$$

is the mean stress in a point being considered whereas

$$\frac{d\rho_0}{d\sigma_m} = \kappa_0 \tag{15b}$$

denotes the coefficient characterizing a change of density of soil exposed to hydraulic pressure $(\sigma_h = \sigma_m)$, and

$$\dot{\varepsilon}_v = \frac{\Delta \dot{V}}{V} \tag{15c}$$

is the rate of dilatational strain measured in triaxal apparatus (Fig. 6a) from the beginning up to the moment of appearance of the limit state in sample (the end of volume decrement). Such results, for loess and clay, are given in [37]. They are based on the rule:

$$\dot{\varepsilon} = 3\Delta\dot{\varepsilon}_1 - \dot{\varepsilon}_\upsilon = 3(\dot{\varepsilon}_1 - \dot{\varepsilon}_h) - \dot{\varepsilon}_\upsilon . \tag{16}$$

where $\Delta\dot{\varepsilon}_1$ stands for velocity of vertical strain of sample, after applying addtional charge, producing the vertical stress σ_1.

The value $\dot{\varepsilon}_h$ refers to the strain ε_h when the hydraulic pressure is applied to the sample, thus $\dot{\varepsilon}_h = 0$ and $\Delta\dot{\varepsilon}_1 = \dot{\varepsilon}_1$. In this way it is possible to calculate

$$\Delta\dot{\varepsilon}_1 = \dot{\varepsilon}_1 = \frac{1}{3}(\dot{\varepsilon} + \dot{\varepsilon}_\upsilon), \quad 2\dot{\varepsilon}_2 = \dot{\varepsilon}_\upsilon - \dot{\varepsilon}_1 . \tag{16a}$$

Let us next locate a soil element of adequate length, with its cross-section (square) equal to that of the sample in the elastic area of the field plowed (Fig. 1c). Let us assume that this element, being in two-dimensional state of strain, possesses the following values of strain rates coinciding with the main strains:

$$\dot{\varepsilon}_{1f} = \frac{\Delta \dot{u}_1}{\Delta l_1'}, \dot{\varepsilon}_{2f} = \frac{\Delta \dot{u}_2}{\Delta l_2'}, \dot{\varepsilon}_{3f} = \frac{\Delta \dot{u}_3}{\Delta l_3'} \cong 0, \tag{17}$$

where: $\Delta l_1', \Delta l_2', \Delta l_3'$ denote initial dimensions of the element being considered and $\Delta \dot{u}_1, \Delta \dot{u}_2, \Delta \dot{u}_3$ correspond to the rate of the local length change. Assuming similar soil properties as well as similar mean stress σ_m and mean strain velocities for both cases:

$$\dot{\varepsilon}_m = \tfrac{1}{3}\left(\dot{\varepsilon}_1 + \dot{\varepsilon}_2 + \dot{\varepsilon}_3\right) = \tfrac{1}{3}\dot{\varepsilon}_v, \tag{17a}$$

one is allowed to use the results of triaxal tests to estimate the thickness of the elastic area, created in front of the share, at similar rates for both processes. It will be done later but firstly some data are presented. The test results for cohesive soil (loess, clay - moisture $12 \div 17.8\,\%$) are as follow [37]: D = 37.6 mm, l = 79 mm (Fig. 5), $\sigma_2 = 0 \div 0.05$ MPa, $\sigma_1 = 0.1 \div 0.25$ MPa for relatively small deformation rates $\left(\dot{\varepsilon}_v \cong 0.05\,s^{-1}, \quad \Delta\dot{\varepsilon}_1 = \dot{\varepsilon}_1 \cong 0.15\,s^{-1}\right)$. For the assumed reasonable piston velocity equal to 0.014 - 0.046 m/s shearing time $\approx$ 0.5 s for $\varepsilon_v = 0.02 \div 0.055$, $\Delta\varepsilon_1 = \dfrac{\Delta l}{l} = 0.13 \div 0.25$ and sample density $\rho = 1.5 \div 1.7$ t/m^3 (reaching 1.88 t/m^3 for moisture value equal to 17.8%). At higher deformation rates the shearing time equals $0.04 \div 0.035$ s and the adequate values are following: for $\dot{\varepsilon}_{Vv} = 0.3 \div 0.5\,s^{-1}, \dot{\varepsilon}_{1v} = 1.7 \div 2\,s^{-1}$, and for $\varepsilon_{Vv} = 0.02 \div 0.048$ $\Delta\varepsilon_{1V} = 0.08 \div 0.18$ (smaller at higher speed) for vertical stresses $\sigma_{1v} \approx 0.2 \div 0.35$ MPa (σ_2 as before).

It should be noted that at higher velocity values the sample deformations are smaller, up to the moment of reaching of the limit state. This proves an existence of strain concentration regions in the samples at higher vertical stresses σ_{1v}. Probably similar phenomena exist during the plowing process. Also the cohesion and the angle of soil internal friction grows up when the piston's speed increases. For the sand these variations are smaller. Additionally some memory effect was observed during other triaxial special tests with repeated vertical loading of the sample [38]. The sample (particularly that of wet clay) submitted to that process had been contracted in volume, independent on some charging-discharging effects

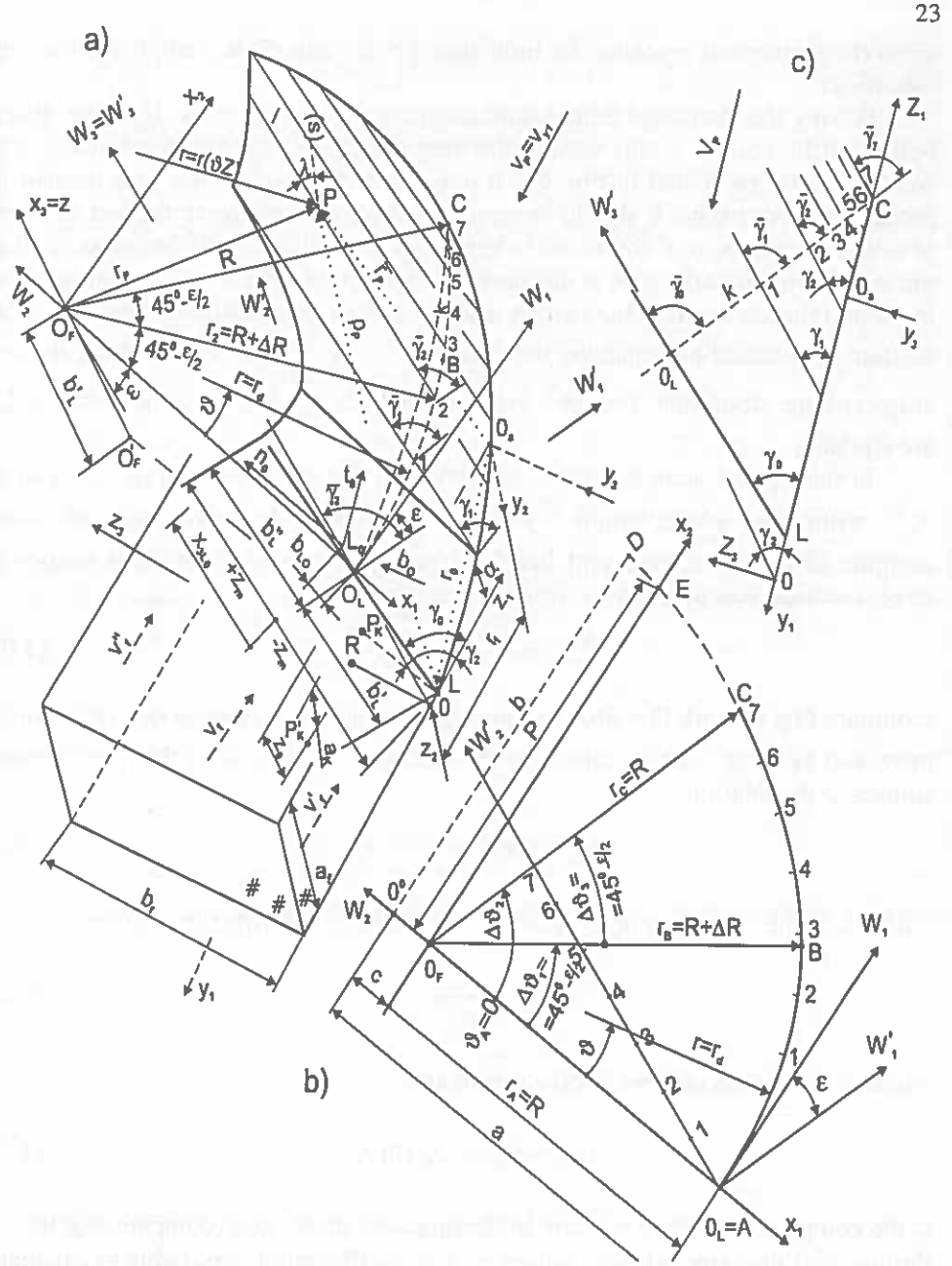

Fig. 2. Directrix and generating lines: a – perspective view, b – construction of directrix, c – generating lines.

up to the moment of reaching the limit state i.e. the end of the sample contraction (shearing).

Having the data cited before, and assuming or testing in the field the distribution of the volume strain rates in the elastic area, in front of the plow bottom, (schematically presented in Fig. 6b) it is possible to estimate the time needed to produce the limit state. It should be measured from the first up to the last moment of volume decrement of field's soil element. It is obtained by the assumption that the work done in both cases is the same and the time for field soil compression is in some relation to that obtained by triaxial test in comparable conditions. This relation is obtained by replacing the $\dot{\varepsilon}_v$ curve by the $\dot{\bar{\varepsilon}}_v$ line representing the average volume strain rate (Fig. 6b); areas under lines $\dot{\varepsilon}_v, \dot{\bar{\varepsilon}}_v$, for some distance l_e, are equaled.

In the triaxial sample on the contrary, the rate of volume strain is equal to $\dot{\varepsilon}_v^{\,tr}$ within the whole length l (Fig. 6a). Assuming the same areas of cross-sections of triaxial sample and field's element, even having different shapes in cross-sections, it is possible to write the relation:

$$\dot{\bar{\varepsilon}}_v l_e \approx \dot{\bar{\varepsilon}}_v \cdot t_e = \varepsilon_v^{\,li} \tag{17b}$$

(compare Fig. 6a with Fig. 6b). It is justified, because the average rate of strain $\dot{\bar{\varepsilon}}_v$ provoked by same average value of stress tensor S (eq. (1)) after the time t_e corresponds to the relation:

$$\varepsilon_v^{\,tr} = \varepsilon_v^{\,li} = \dot{\varepsilon}_v^{\,tr} \cdot t_{tr}, \tag{17c}$$

where t_{tr} is the time of sample shearing. The variable t_e fulfils the relation:

$$t_e = \frac{l_e}{v_{pe}}, \tag{17d}$$

where l_e is a length of field's soil element and

$$v_{pe} = v_{w_1'} = v_p \sin\gamma_2 \tag{17e}$$

is the component of plow velocity in the direction of w_1' axis (compare Fig.1c). Putting next the same relation, where n_e is a coefficient, it is possible to calculate the time:

$$\dot{\varepsilon}_{\upsilon} \Big/ \dot{\varepsilon}_{\upsilon v}{}^{tr} = \left(\frac{\upsilon_{pe}}{\upsilon_{pist}} \right)^{n_e} \tag{17f}$$

$$t_e = \left(\frac{\upsilon_{pe}}{\upsilon_{pist}} \right)^{n_e} t_{tr} \tag{17g}$$

which is necessary to provoke the field's element to be sheared off starting from the beginning of compression up to the end of volume element contraction. The plow bottom is then transferred for the distance representing a length of the elastic area in field. It allows us to calculate the formulas for the linear strain rate at the end of the elastic state for the problem being considered. They have the following final form:

$$l_e = \upsilon_{pe} \cdot t_e = \left(\frac{\upsilon_{pe}}{\upsilon_{pist}} \right)^{n_e} t_{tr} \cdot \upsilon_p \cdot \sin \gamma_2 = \frac{\left(\upsilon_p \sin \gamma_2 \right)^{n_e+1}}{\left(\upsilon_{pist} \right)^{ne}} \cdot t_{tr} \tag{18}$$

It allows us to calculate the linear strain rate at the end of elastic state:

$$\dot{\varepsilon}_{w_1'}{}^{el} = \dot{\varepsilon}^{li}{}_{w_1'} = \left(\frac{\upsilon_{pe}}{\upsilon_{pist}} \right)^{n_1} \dot{\varepsilon}_1^{tr}, \tag{19}$$

where n_1 denotes an empirical coefficient and $\dot{\varepsilon}_1^{tr}$ represents the rate of vertical strain for sample shearing in triaxial test at higher speed. For example admitting that $n_e = n_1 = 1/2$, one receives $t_e = 0.05$ s and the dimension of area in the direction of the w_1' axes as the value equal to $l_e = 1.24 \times 0.04 \times 5.4 \times 0.62 \approx 0.054$ m for $\dot{\varepsilon}^{li}_{w_1'} = 1.24 \times 2 \cong 2.48\, s^{-1}$ from the following assumptions:

$$\dot{\varepsilon}_1^{tr} = 2 s^{-1}, \quad t_{tr} = 0.04 s, \quad \frac{\upsilon_{pe}}{\upsilon_{pist}} = \frac{1.4 \sin 38^0}{0.55} = 1.56$$

$$\upsilon_p = 1.4\, m/s \cong 5\, km/h, \quad V_{pist} = 0.55\, m/s, \quad \gamma_2 = 38^o \tag{19a}$$

When the soil reaches the limit state then $\dot{\varepsilon}_{\upsilon}$ becomes zero and the first shear surface appears. At that moment some soil elements possess the linear strain $\varepsilon^{li}_{w_1'}$, which next grow up (curve ε behind the point L_i with strain rate $\varepsilon^{pl}_{w_1'}$) having practically constant value; neglecting some changes provoked by the increase of stresses caused by a growth of the clod thickness. The soil element transfer

from the elastic to plastic state takes place when the conditions defining the limit state are fulfilled [1,6,31]. These conditions for soil being in the so-called full plastic state are described by Haar-Karman's hypothesis [35,46] valued when two of the main stresses are equal to each other i.e.

$$\sigma_1 = \sigma_3 > \sigma_2 \text{ or } \sigma_1 > \sigma_2 = \sigma_3 \tag{19b}$$

giving two limit conditions. In another case it is impossible to receive a solution for the problem of the limit state, without additional assumptions, concerning the physical aspect of soil deformation problem. Then the relation given by eq. (1) is not valued. Instead of this some another relation should be introduced describing the stress conditions at the limit state. For soil medium it's convenient to apply Coulomb-Mohr's hypothesis giving the dependence of shear stresses from the normal stresses, which in a general form is:

$$\tau = f(\sigma). \tag{20}$$

However further, for cohesive soil, a simple commonly known equation is applied:

$$\tau = c + \sigma_n \operatorname{tg}\phi, \tag{20a}$$

where c denotes cohesion, and ϕ - angle of soil internal friction (adequate for the speed of the process being considered). During the time when the soil element is subjected to the stress adequate for the limit state, those stresses are fulfilling the motion equations, which are received from the equation (2), by rewriting into separate components (presenting Cauchy's equations) [26,41]:

$$\rho(a_k - F_k) = \frac{\partial \sigma_{kr}}{\partial x_r}. \tag{21}$$

For slow processes $(a_k \cong 0)$ they become equilibrium equations. The solution of such equations, if it is to be found in a particular case, respecting the continuity equation (3a) where $\operatorname{div}\vec{v} = 0$ as well as boundary and initial conditions leads to a determination of the shear surfaces in some area, [35,40,46]. But this problem is difficult in realization and in many cases it is suggested [6] to draw a pattern of expected slip lines, fulfilling certain conditions, than to check it.

This procedure is applied further, together with accompanying simplification, acceptable from the technical point of view. Some details of the problem are also separated (Fig. 7) and discussed individually. Thus the clod, as mentioned in second chapter after cutting off (Figs 7b,f) undergoes separation from the field along the side wall surface $L_0'O_a N_1'$ (Figs 7a,d). It is separated also along the

whole front shear surface $L_0'N_1'N_1''L_0''$ (Fig. 1a) and next is being pushed to the moldboard with some relative speed υ_{fB}. This speed will be decomposed into three components, defining the clod's transverse speed $\upsilon_{\vartheta B}$, radial speed υ_{rB} and also its displacement speed υ_{zB} along the z-axis.

CLOD FORMATION AND MOTION OVER MOLDBOARD

The clod possesses an elastic area at the head, next the plastic one with the shear surfaces, where an effect of crushing, bending and shearing appears [6] crossing the upper clod surface at the angle 45^0-$\phi/2$. It vanished on the last line (surface $L_1'L_1''K_1''K_1$) presumably starting between the middle and the end of the share. Over there intensive clod deformation takes place, going on with the rate of linear strain $\dot{\varepsilon}_{w}^{pl}$ (Fig. 6c) within the time dependent on the length of that area; bigger in the upper part.

These phenomena are responsible for the crushing process and the time of clod deformation and in that way also for the clod's thickness growth and soil mass transfer in the field. The linear strain deformation rate $\dot{\varepsilon}_{w_1}^{pl}$ may be estimated by assuming that it has a constant value in the whole plastic area of the medium length l_{pm}, but the dimensions and the strain rates distribution in that area are not known. They depend on many factors and require special investigations.

It can be assumed here, that the medium length of the plastic area l_{pm} is equal approximately to the clod thickness a_c in that area. For a practical purpose, it is also convenient to include a half of the length of the elastic area $l_e/2$ into the mentioned area (eq. (18)) possessing the rate of linear strain $\dot{\varepsilon}_{w_1}^{pl}$ - (eq. (19)), Fig. 6c. This procedure allows us to estimate the velocity decrement in both areas: elastic and plastic having a substitution medium length (Fig. 7e):

$$l_{ep} = \frac{1}{2} l_e + l_{pm}. \tag{22}$$

Behind the plastic area $L_1'L_1''K''K'$, (Fig. 1a) the elastic area with decreasing tensions appears again.

In the rear part of the clod there may sometimes appear an area indicating a phenomenon of slope sliding along the surface $T_1 T_2 E E_2$. Such problem can be, to some extend, solved as a slope stability problem by defining the slope line using a simplified Sienkov's formula [14], written in a moving coordinate system. Here, for simplicity, it is assumed that the clod sustains its movement up to a moment of arriving at the end of a moldboard, suspending its dimensions received at the end of the plastic area. That part of clod of the length l_{pp} behaves like a granular medium subjected to the action of forces discussed later. The clod de-

formation in that area is practically equal to zero. Its motion is smooth providing sliding effects does not destroy it. Such effect, typical for dry sand, causes the clod thickness increase and disturbs the clod's proper movement. The process is getting similar to that observed in the action of bulldozer blade inclined at an angle to the direction of motion. However this problem is behind our considerations.

The soil particles located near the implement surface, subjected to the process possess at the beginning the relative speed $\upsilon_b = -\upsilon_p$ equal to the plow speed but turn in the opposite direction, next taken as $|\upsilon_b|$. This speed is decomposed into three components as it was mentioned before. One component corresponds to the direction $w_3' = z$ (Fig. 1a):

$$\upsilon_{w_3'b} = \upsilon_{zb} = \upsilon_p \cos\gamma_2, \tag{23}$$

next one has the direction compliant with w_1' axes (transverse speed in Fig. 1 c):

$$\upsilon_{w_1'b} = \upsilon_{\vartheta b} = \upsilon \sin\gamma_2 \cos\varepsilon, \tag{23a}$$

and third one is the radial speed parallel to the w_2' axes:

$$\upsilon_{w_2'b} = \upsilon_{rb} = \upsilon_p \sin\gamma_2 \sin\varepsilon. \tag{23b}$$

The angle γ_2 stands here for the second generating line (see Fig. 4) representing an average inclination value for the soil particles moving near the centers of clods' cross-section. It is assumed that component υ_z in the elastic and plastic area does not change its value because of soil deformation, as the considered soil element during translation does not change its length in that direction: $(\varepsilon_z = \varepsilon_{w_1'} = 0)$, certainly neglecting some discrepancies. Both components $\upsilon_{\vartheta b}$ and υ_{rb} change their value at the beginning of the process near the implement surface mainly due to the direction change, but the length of the resultant velocity is preserved (Fig. 8): $\left|\vec{\upsilon}^{\,b}_{w_1'}\right| \cong \left|\vec{\upsilon}_{w_1'b}\right| = \left|\vec{\upsilon}_{\vartheta b} + \vec{\upsilon}_{rb}\right|$. The soil deformation can be considered in another way presented in Fig. 8c. The plow bill L approaches the soil with the velocity υ_p being the transportation velocity υ_{tr} of the soil particle moving parallel to the landside cutting edge with the relative velocity υ_{re}.

We will further consider the situation when the soil element placed in the field along the w'_1 axes would have the length l_ϑ (measured in the direction of ϑ coordinate). It would, after deformation in the range of elastic and plastic area, decrease for the length l_{ep} (eq. (22)); measured as an arc in the center of clod:

$$l_{ep} = \frac{1}{2} l_e + l_{pm} = l_\vartheta - \Delta l_\vartheta \cong l_\vartheta\left(1 - \dot{\varepsilon}_1 t_{ep}\right), \tag{24}$$

where $\dot{\varepsilon}_1 = \dot{\varepsilon}^{pl}_{w_1}$ denotes the linear strain rate of soil plastic deformation.

Thus the adequate length in the field in the direction of implement motion (y_1), before soil deformation starts, would have the value:

$$l_{y_1} = \frac{l_g}{\sin\gamma_2} = \frac{l_{ep} + \Delta l_g}{\sin\gamma_2} \cong \frac{l_{ep} + \dot{\varepsilon}_1 t_{ep} l_{ep}}{\sin\gamma_2} \tag{24a}$$

where γ_2 is the inclination angle of 2nd generation line (Fig. 4). Hence the time of clod's soil particles presence in the elastic and plastic area is:

$$t_{ep} = \frac{l_{y_1}}{\upsilon_p} = \frac{l_{ep}}{\upsilon_p \sin\gamma_2 - \dot{\varepsilon}_1 l_{ep}}. \tag{24b}$$

The clod thickness at the end of this process can be estimated after assuming two-dimensional state of clod deformation (Fig. 1c) and applying the continuity equation in a simple form ($\dot{\varepsilon}_V = 0$). Thus

$$\dot{\varepsilon}_1 + \dot{\varepsilon}_2 \cong -\frac{1}{t_{ep}}\frac{\Delta l_{ep}}{l_{ep}} + \frac{1}{t_{ep}}\frac{\Delta a_c}{a_c} = 0\,. \tag{24c}$$

Then $\dot{\varepsilon}_1 = -\dot{\varepsilon}_2$ and the clod thickness increment is:

$$\Delta a_c = \frac{\Delta l_{ep}}{l_{ep}} a_c = \dot{\varepsilon}_1 t_{ep} a_c = \frac{1}{\kappa_\gamma}\dot{\varepsilon}_1 a_f\,, \tag{24d}$$

where the following notation was used: a_f represents the depth of plowing whereas the coefficient of clod pulverization κ_γ together with the clod thickness a_c after time t_{ep} can be calculated on the basis of the following equations:

$$\kappa_\gamma = \frac{\gamma_c}{\gamma_f} \tag{24e}$$

$$a_c = a_f\left(1 + \frac{1}{\kappa_\gamma}\dot{\varepsilon}_1 t_{ep}\right). \tag{24f}$$

The particle velocity υ_g, having the value υ_{gb} (eq. (23a)) at the beginning would drop down its value dependent on the position of point being under consideration

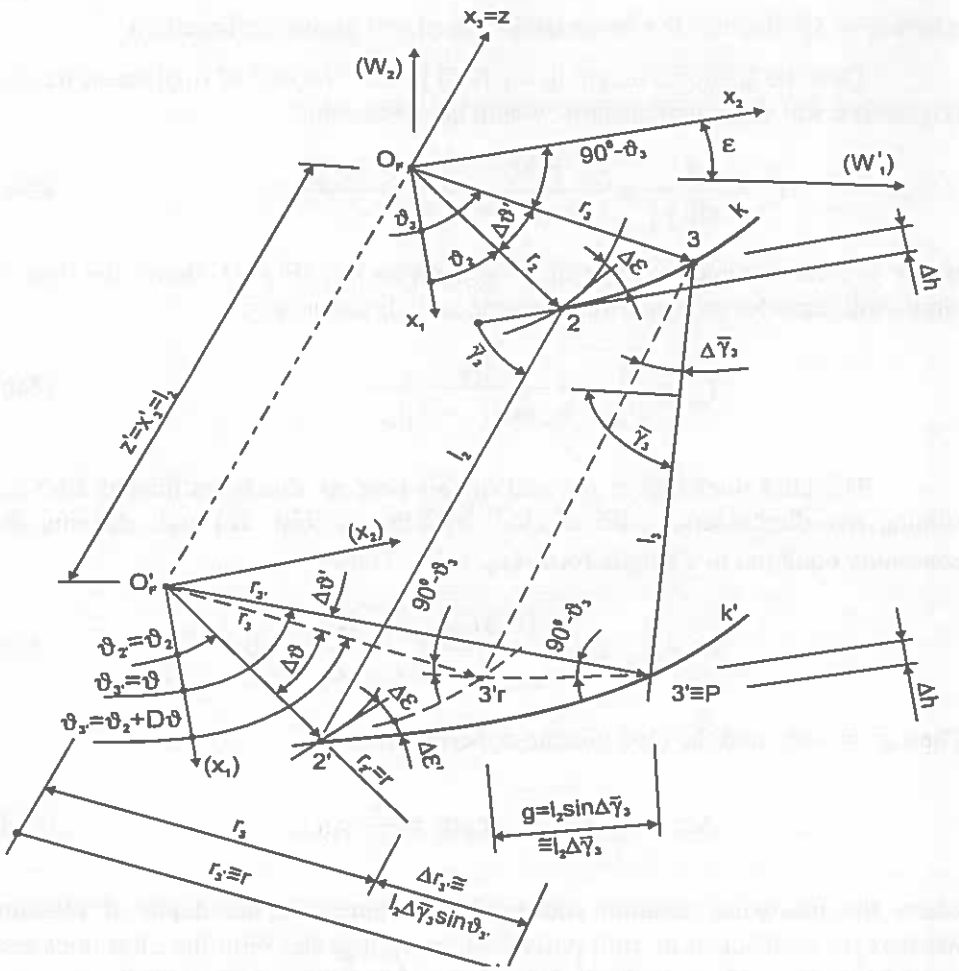

Fig. 3. Plow board surface in cylindrical coordinates $O_F r \vartheta z$.

(time of deformation) in accordance to the formula:

$$\upsilon_{w_1} = \upsilon_{w_1 b} - \dot{\varepsilon}_1 \Delta w_1 \cong \upsilon_\vartheta = \upsilon_{\vartheta b} - \dot{\varepsilon}_1 r_s \vartheta \tag{25}$$

In this equation $\dot{\varepsilon}_1$ stands for the linear strain rate in the ϑ direction, Δw_1 is clod length dependent on the time of process duration, which had been already run,

$$\Delta w_1 \cong \Delta w_\vartheta = \upsilon_{\vartheta_1} \Delta t \tag{25a}$$

where υ_{ϑ_s} is the velocity component in $t_\vartheta \cong \vartheta$ direction (tangent to the implement cross-section in the plane traced by coordinate ϑ (Fig.1a), r_s - radius of the center of clod's cross-section at a certain moment. However for plastic area (e.g. B_1B_k in Fig. 7g)

$$\Delta t = t_p, \quad \Delta \upsilon_\vartheta = l_{pm} \cong a_c . \tag{25b}$$

Considering the clod formation we do not know the distribution of velocity components just after this process starts. That is the reason, among others, for the simplifications introduced. Thus, the soil's speed component υ_z does not depend on soil deformation in the area of elastic and plastic deformation in the z-direction. It only depends on the angle λ of resultant speed inclination to the generating lines, discussed later. But the soil velocity component υ_ϑ in the ϑ direction in the area mentioned changes its direction and also its value in accordance with a certain equation (see eq. (24)). The resultant velocity of two above mentioned components (υ_z , υ_ϑ), refereed to the radius r_s, is expressed by the following formula:

$$\upsilon_s = \sqrt{\upsilon_z^{\,2} + \upsilon_\vartheta^{\,2}} \cong \upsilon_p \sqrt{\cos^2\gamma_2 + (1 - \frac{\dot{\varepsilon}_1 r_s \vartheta}{\vartheta_p \sin\gamma_2})^2 \sin^2\gamma_2} \tag{26}$$

It changes its value depending on the ϑ angle, in reference to time t_{ep} (see eq. (24a)), being the time of soil particle existence in the elastic and plastic areas. During the plowing process the clod's particles rotate around the z-axis with angular speed:

$$\omega_z = \frac{\vartheta - \vartheta_o}{t - t_o} = \frac{\upsilon_{\vartheta s}}{r_s} \tag{27}$$

changing its value with time (index „s" refers here certain value to the center of the clod cross-section); t is the time of process measured from beginning ($t = t_0$). For example assuming the clod length being considered: plowing speed: $\upsilon_p \cong 1.4$ m/s, rate of linear strain: $\varepsilon_{w_1}^{Li} \cong \dot{\varepsilon}_1 = 2.48$ m/s,

$$\begin{aligned} &\Delta w_1 \cong r_s \vartheta = l_{ep} = \frac{1}{2} l_e + l_{pm} = \frac{1}{2} 0.054 + 0.2 \cong 0.227m, \\ &l_e = 0.054 \quad l_{pm} \cong a_c \cong a_f = 0.2m \end{aligned} \tag{27a}$$

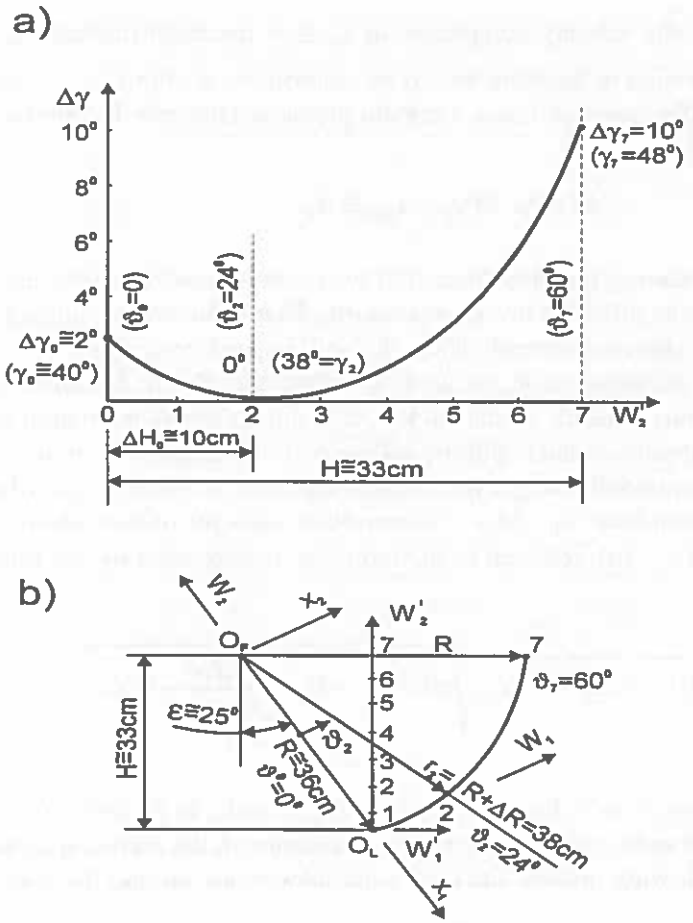

Fig. 4. Changes of moldboard parameters: a – angle γ, b – radius r.

$$\text{angle: } \gamma_2 = 38^o \text{ (Fig. 4a)}, \varepsilon = 25^0 \tag{27b}$$

$$\text{radius: } r_s \cong r_2 - \frac{1}{2}a_f = 0.38 - \frac{1}{2}\cdot 0.2 = 0.28m \text{ ,(Fig.4b).}$$

Then one receives from equation (26) the mean speed of clod in the elastic and plastic areas: υ_z=1.22 m/s and time t_{ep} = 0.159 s. From here we get the component in the z-direction $\upsilon_z = 1.22\cos 38^0 = 0.96$ m/s. Then after some calculations the component in the ϑ direction equals: $\vartheta_\vartheta = 0.68$ m/s (compare eq. (23) and (23a)) and finally $\omega_z = {}^{0.68}\!/_{0.28} = 2.43$ s^{-1}.

Except that rotation the clod possesses also some additional rotation ω_c around the temporary center of rotation O_l laying down right from the end of the share (Fig.1a). It happens due to different soil deformation caused by the stresses acting there in certain time and evokes a different rate of deformation at the left and the right side of the clod $(\dot{\varepsilon}_1' \langle \dot{\varepsilon}'')$. At the right side of clod, in the plastic and elastic areas, the value of stress tensor is higher than at the left side. It happens because the right side of the clod is thicker and the soil particles go up there steeper to the moldboard then at the left side.

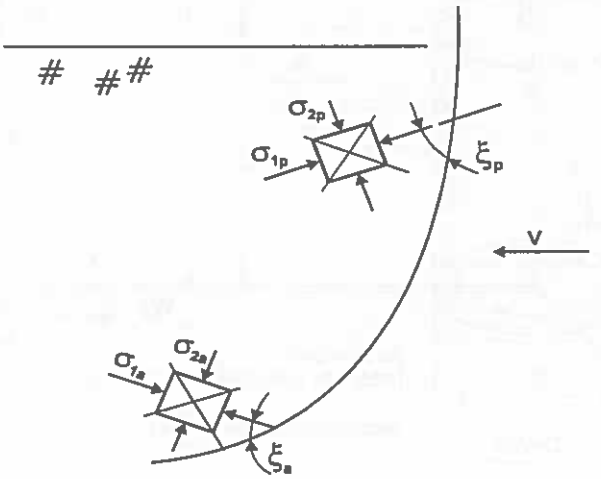

Fig. 5. Inclination of the biggest main stresses in the active and passive states.

The process of this action as well as the stress and pressure in the soil mass engaging the plow bottom is not yet satisfactorily known [10]. Some magnitude of deformation's rate difference between the two sides of clod in the mentioned area can only be assumed. Then we can write a relation of clod rotation (ω_c) around the temporary point O_c, located at the distance r_f'' from the end of the shear (Fig. 1a):

$$\omega_c = \frac{\upsilon_c'' \sin \lambda_o}{r_f''} = \frac{\upsilon_c' \sin \lambda_o}{r_f'' + b_L'' + b_L'} . \tag{28}$$

The values υ_c' and υ_c'' stand for the speeds of clod particles moving in the planes coinciding with the right and left wall of clod whereas $\upsilon_c' \sin \lambda_o$, $\upsilon_c'' \sin \lambda_o$, are interrelated with the eq. (23a), replacing there υ_p by υ_c' or υ_c''. The value λ_0 stands here for the inclination angle of the resultant speed $\upsilon_b = |\upsilon_p|$ against the z-axis and it can be described by the following formula:

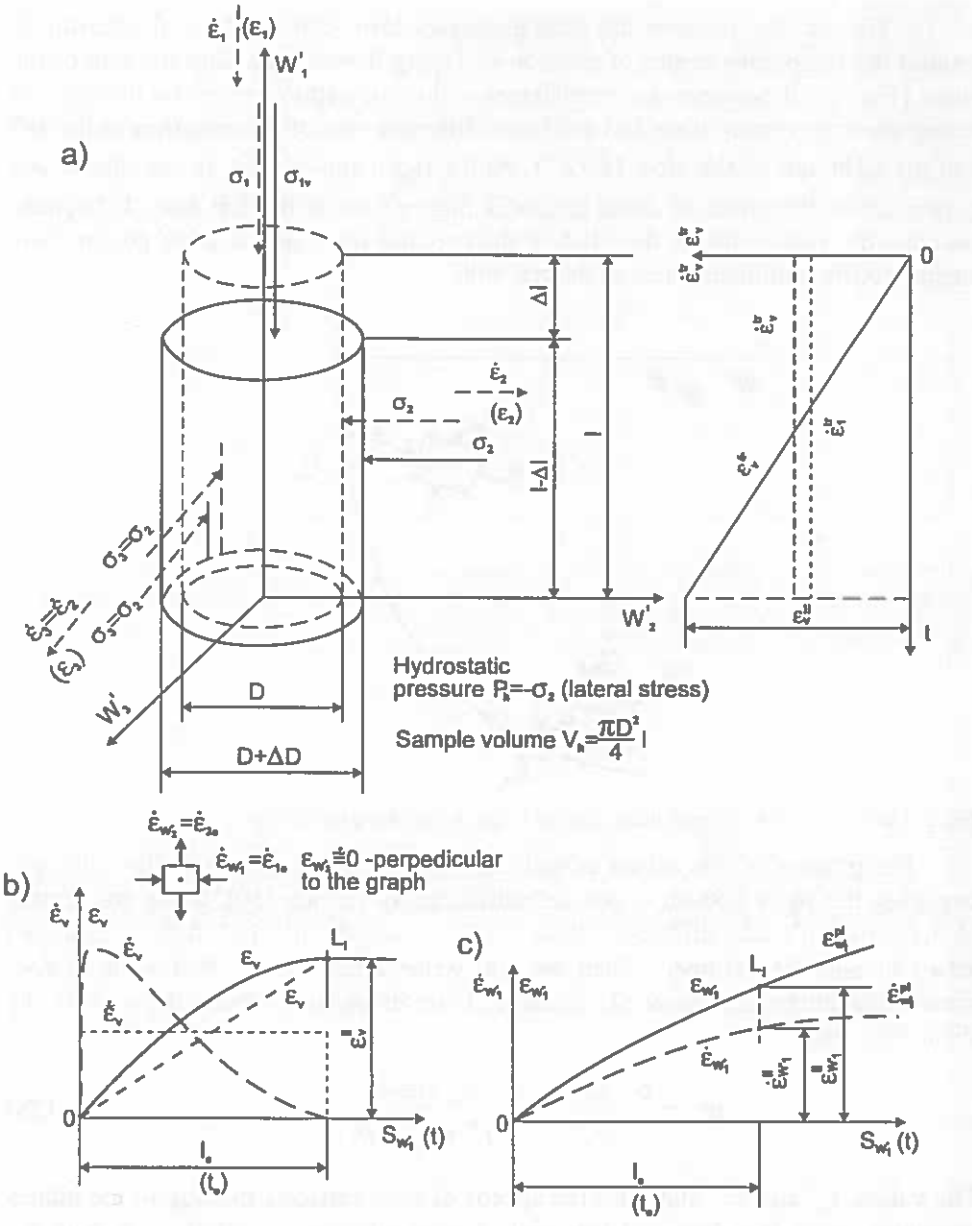

Fig. 6. Comparison of triaxial sample deformation with subsoil deformation in elastic area: a – sample compression in triaxial apparatus, b – volume deformation of field element, c – longitudinal deformation in field.

$$\operatorname{tg}\lambda_o \cong \frac{\operatorname{tg}\gamma_2}{\cos\varepsilon}, \tag{29}$$

where γ_2 is given in Fig.4, for the directrix line placed near the share-moldboard junction. For example assuming $\gamma_2 = 38^0$, $\varepsilon = 25^0$, one gets $\lambda_0 = 42^0$. Next assuming: $\upsilon_c'' = 0.7\frac{m}{s}$, $\upsilon'_c = 0.9\frac{m}{s}$, $b_f = 0.3m$, $b_L'' + b_L' = {}^{b_f}\!/_{\sin\gamma_2} \cong 0.485$ m we can get $r_f'' = 1.7m$, $\omega_c = 0.28$ s^{-1}. It amounts to about 9% as compared with $\omega_2 =$ 3.15 s^{-1} (see eq.(27)).

During the deformation process a clod element, being placed at the center of clod's cross-section B (Fig. 8), has the velocity υ_{sr} which later changes its value and its direction. At the beginning it had the value υ_{sf} and the initial direction represented by some unit tangent vector t_f (Fig.8). It changes its direction for any other direction represented by unit vector e.g. t_r (point B). Those unit vectors being tangent to a motion trajectory at a certain moment, for the element being considered, together with other unit vectors (n - normal, b - binormal) make a base of unit vectors, characterizing a spatial curve [7,18,47].

In our case the initial direction of the unit vector t_f is parallel to the plow velocity but oriented in the opposite direction. In the area of soil deformation, that unit vector, presenting the direction of soil particles' motion, changes its direction. We assume, that just after beginning the tangent unit vector t_r, still representing the direction of the velocity vector of soil particles $\upsilon_{ab} = -\upsilon_p$, is parallel to the side edge of the plow bottom. It defines the initial inclination angle λ_0 (eq. (29)) of the soil particle velocity in reference to the generating lines (measured of course on the plow bottom surface).

Two other unit vectors (n_r, b_r) describing the flexion (bending) and torsion of soils' particles trajectory line, being a part of some degenerated screw line, are combined with the t_r vector. The angle λ_0 changes its value (together with the unit vectors - t,n,b) for another value λ dependent on the point being considered and the time of process duration, which is presented in Fig. 8 and inFig.1a - point P. In order to describe this process some equation of soil particle motion trajectory ought to be found, which is done in the next chapter.

However, there are additionally given formulas describing the components of velocity vector υ, for some radius r changing its value and direction, laid down in a rectifying plane [10,18,47]. It is traced by the tangent unit vector t and the unit binormal vector b, for a certain point P (Fig. 1a) of the trajectory line (s). The component of velocity vector paralel to the z-axis is:

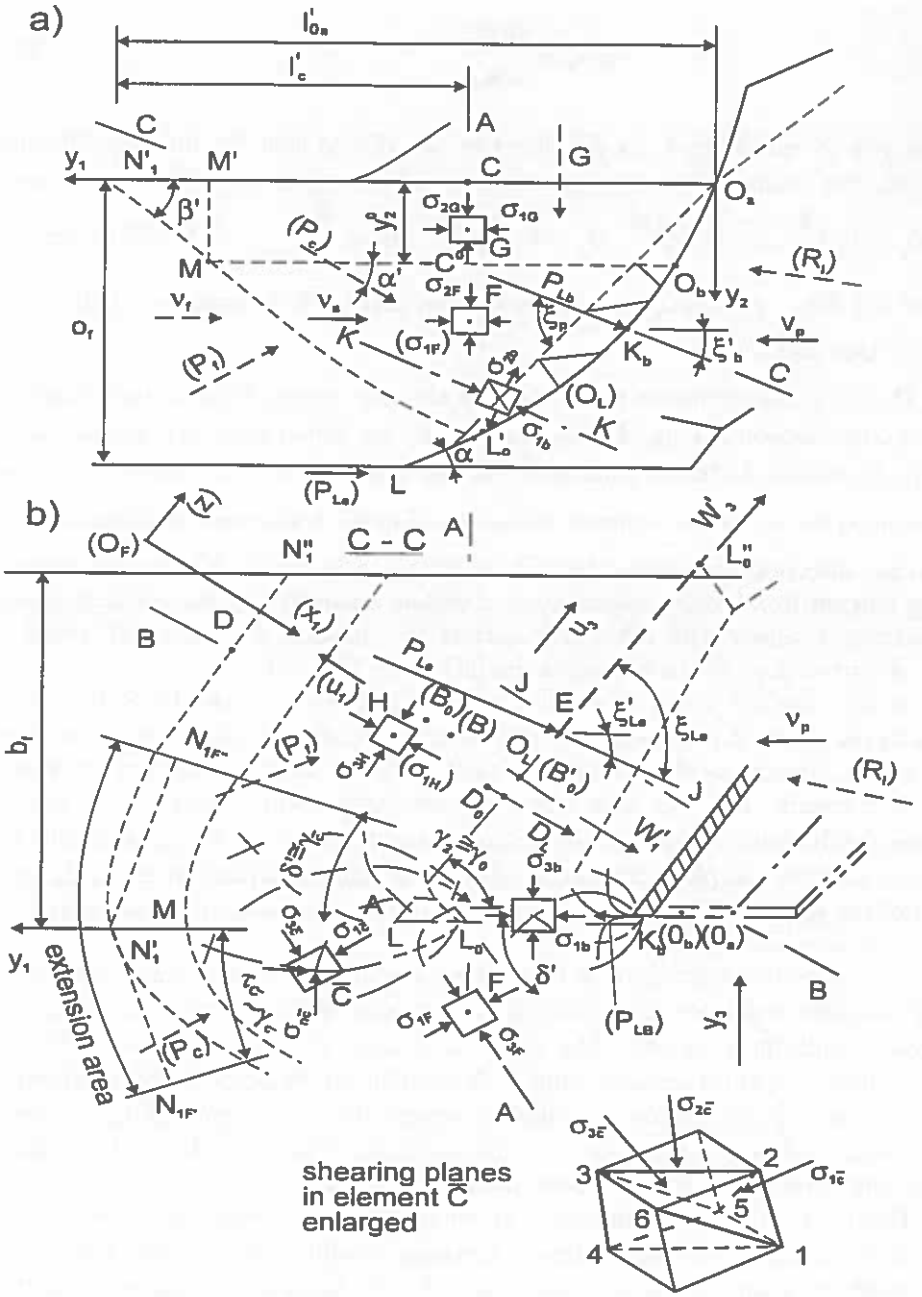

Fig. 7. Clod formation: a – side view, b – projection C – C.

$$\upsilon_z = \upsilon \cos \lambda . \tag{30}$$

According to our assumption during the clod's element translation it is not changing its value due to soil deformation in the elastic and plastic areas. The component velocity vector in the ϑ-direction is:

$$\upsilon_\vartheta = \upsilon \sin \lambda . \tag{31}$$

It changes its value according to the relation (25) for a certain radius r. The angle λ decreases its value due to different velocity of particle motions at the right and left side of the clod. This phenomenon is described by the vector of clod rotation ω_c, expressed by eq. (28). Thus the range of decrement of the λ angle (in elastic and plastic areas) is given by following formula [41]:

$$\lambda = \lambda_o - \omega_c\left(t - t_o\right), \tag{32}$$

where λ_0 is given by the eq. (29), t is the time of plowing process from the beginning of process t_0. The time t of the plowing process for a certain soil particle depends on its position i.e. the distance z_0 (Fig. 2a), at the beginning ($t = t_0$) from the directrix plane ($z = 0$) traced by points $O_F O_L C$ (Figs. 1a, 2a). Thus, the time t_0 is the so-called lag-time, for a certain particle, laying just above the share edge, at the distance z_0 from the directrix plane; assuming the sign for z_0:

$$t_o = \frac{z_o}{\upsilon_p \cos \gamma_2} . \tag{33}$$

Taking into account the position of another point e.g. point R (Fig. 7e) in the plane $z = 0$ for the distance l_{Ra} from the plastic area at depth a_R the delay time is:

$$t_R = \frac{l_{Ra}}{\upsilon_p \sin \gamma_2} \cong \frac{l_R - a_R \operatorname{ctg}\left(45^o - \dfrac{\phi_f}{2}\right)}{\upsilon_p \sin \gamma_2} . \tag{33a}$$

Thus the total lag-time necessary to pass the part of soil being considered, represented by point R (Fig.7e) located at the distance z_0 from the directrix plane effectively engaged in the plowing, process is to be equal to:

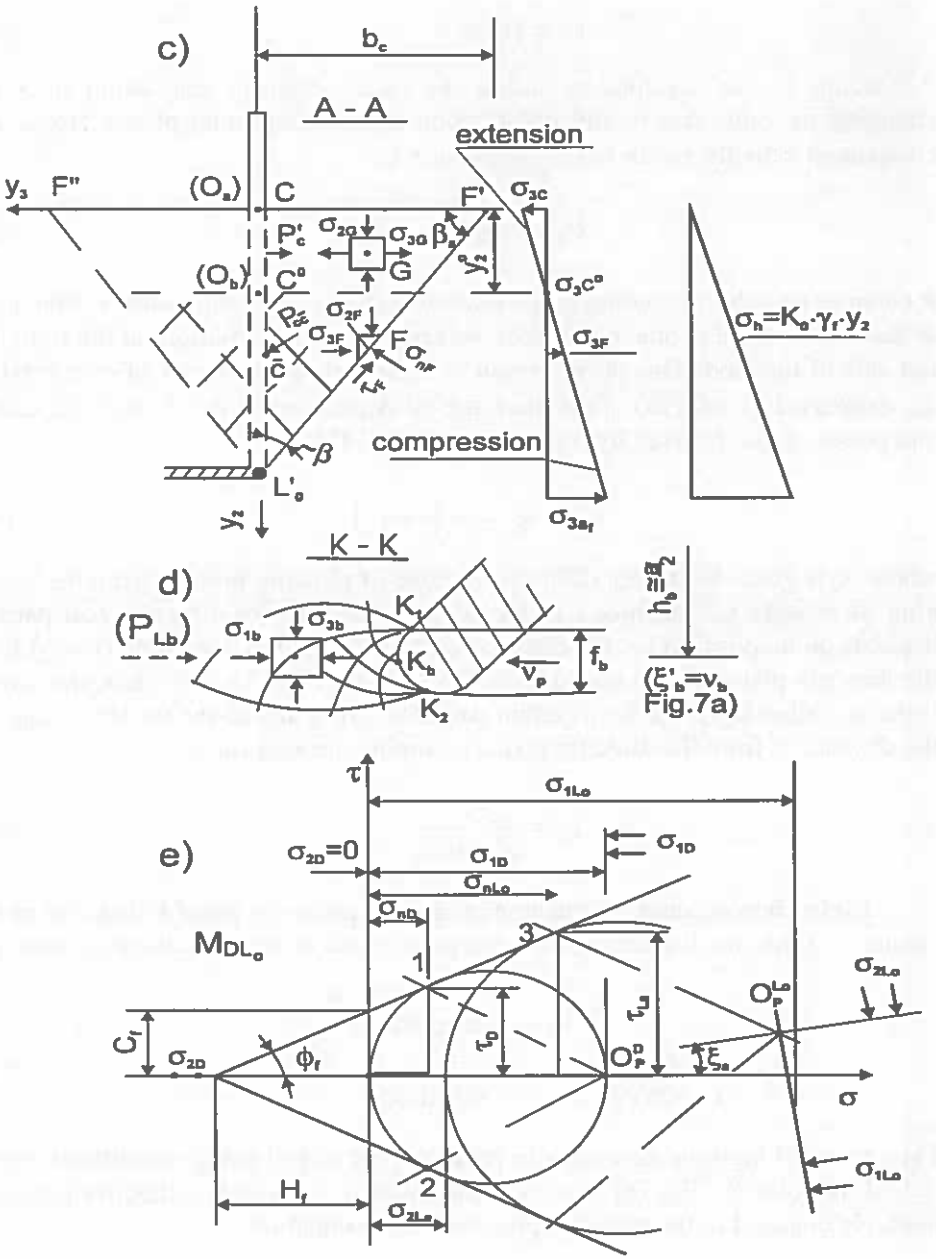

Fig. 7. (Cont.): c – projection A – A, d – action of side edge cross section K – K (see Fig. 7a), e – Mohr's circles M_{DL_0} in points D and L_0 (see Fig. 7g).

For some points (left upper part of the clod) it can have a negative value, but a positive one for points placed right and near from the bottom of the furrow. The clod particle motion behind the plastic area (post-plastic length l_{pp} - Fig. 7e) is not exactly known. For that reason it is to be considered in the same way as at the end of the plastic area, i.e. the clod speed $\upsilon_{spp} = \upsilon_{sk}$ (Fig. 8) and rotation ω_c (eq. (28)) are the same along the trajectory length l_{pp}. However the speed components change theirs values, dependent on the angle according to the formulas (30) and (31), and this component is related here to the clod's central line:

$$\upsilon_{zpp} = \upsilon_{spp} \cos\lambda\,, \tag{34}$$

$$\upsilon_{\vartheta pq} = \upsilon_{spp} \sin\lambda\,. \tag{34a}$$

Rotation speed around the z-axis changes its value along the trajectory line depending on the time t which is given by:

$$\Delta\omega_{zpp}(t) = \omega_{zt}(t) - \omega_{zpp} < 0\,, \text{ for } \{\upsilon_\vartheta : \omega_{zt}(t) < \omega_{zep}\}. \tag{34b}$$

In this equation ω_{zep} is the clod particle rotation speed at the end of the elasto-plastic area (point k, Fig. 8, eq. (27)). Then the following relation gives the rotation speed:

$$\begin{aligned}\omega_{zt}(t) &= \omega_{zep} + \Delta\omega_{zpp}^{(t)} = \omega_{zep} - \frac{\Delta\upsilon_{\vartheta t}}{r_{kpp}} = \\ &= \omega_{zep} - \frac{\upsilon_s}{r_{kpp}} \sin[\lambda_0 - \Delta\lambda_k - \omega_{cpp}(t - t_k)]\end{aligned} \tag{35}$$

where $\Delta\lambda_k = \omega_c(t_k - t_0)$.

is the difference between the angle λ (eq. (32)) and the angle λ_0 related to the point k whereas $\omega_c \cong \omega_{cpq}$ and the radius $r_{kpp} \cong r_k$ can be often taken constant for post-plastic area. The time interval $t - t_k$ equals to:

$$\Delta t_{pp} = t - t_k = \frac{s(t) - s_k(t_k)}{\upsilon_s}, \tag{35a}$$

where $s(t) = s$ is a trajectory line described later and υ_s (eq. (26)) – velocity of a chosen particle. Considering above the formula (35) takes the form:

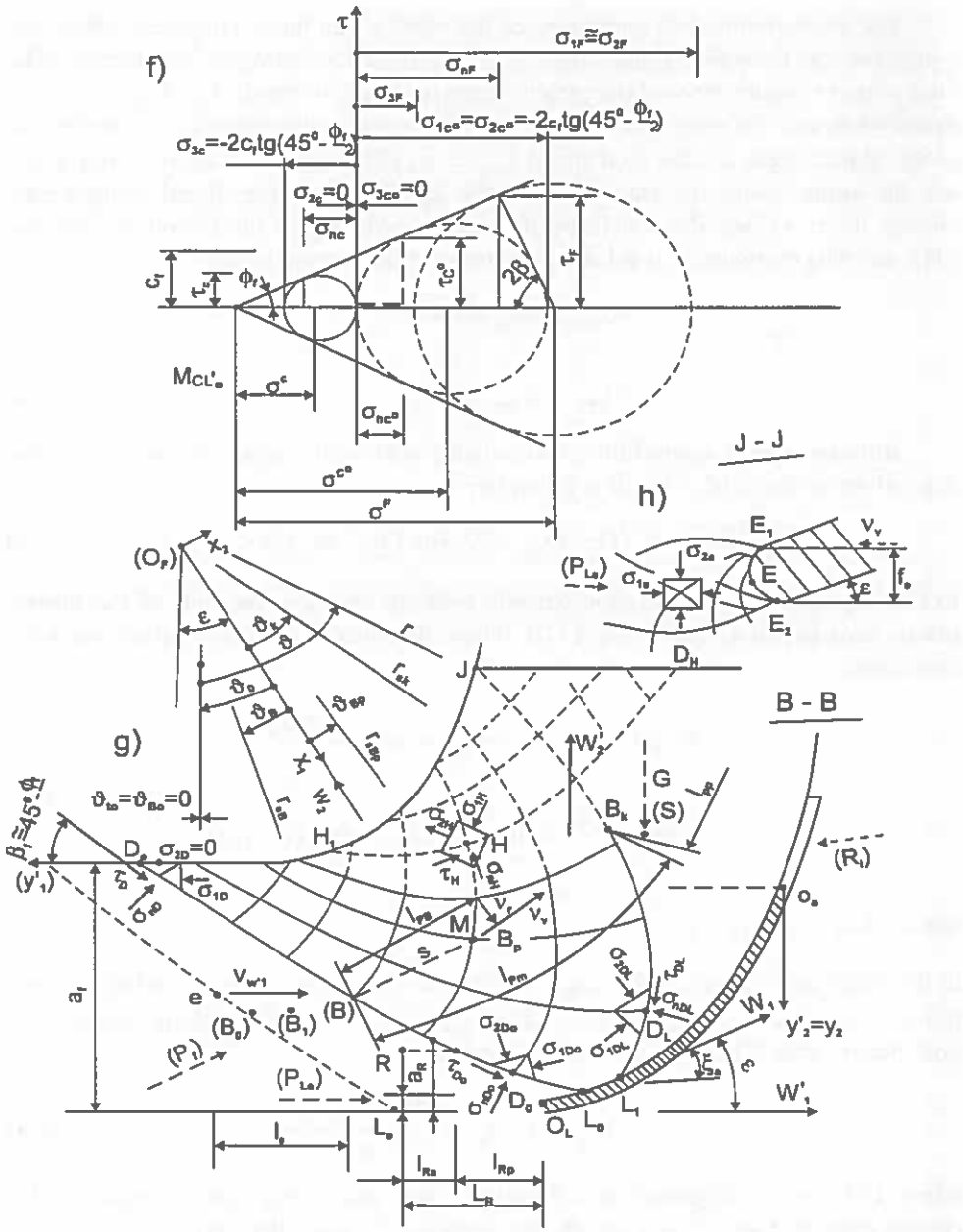

Fig. 7. (cont.): f – Mohr's circles $M_{CL_0'}$ for the vertical plane CL_0' cf. Fig. 7c) , g – clod separation cross section B - B, h – cutting edge cross section J – J (see Fig. 7b).

$$\omega_{zl}(s) = \omega_{zep} - \frac{\upsilon_s}{r_k}\sin[\lambda_0 - \Delta\lambda_k - \frac{\omega_{cpp}}{\upsilon_s}\Delta s_{oc}], \qquad (36)$$

where $\Delta s_{oc} = s - s_k$ is any optionally chosen trajectory length which can be divided into few parts for the calculation reason.

Sometimes, for simplification, the clod motion is related to the clods central line within the time of clod-implement contact from point *M*. to the end *E* (Fig. 8) as a unity motion conserving all plowing parameters existing at the end of the elasto-plastic area. Now we introduce a parameter

$$u = \vartheta - \vartheta_0 = \omega_{zm}(t - t_0), \qquad (37)$$

where the index "0" refers the ϑ and t values to the beginning of the process whereas the value ω_{zm} (eq. 27) is related to the symbols ω_{zl} (see eqs (35), (36)) and to the centers of the clod cross-sections. Assuming

$$t_k \cong t_0, \quad \Delta\lambda_k \cong 0, \quad \omega_{zep} \cong \omega_{zk} \qquad (37a)$$

we can receive:

$$\omega_{zm} \cong \omega_{zk} - \frac{\upsilon_s}{r_k}\sin[\lambda_o - \frac{\omega_{cpp}}{\upsilon_s}\Delta s_{0c}]. \qquad (37b)$$

The time necessary to obtain a position ϑ by a clod's part is:

$$t(\vartheta) \cong \frac{\vartheta - \vartheta_0}{\omega_{zm}} + t_0. \qquad (37c)$$

The angle ϑ related to the lag-time t_{0R} (eq. (33b)) is defined by:

$$\vartheta_{0R} \cong \omega_{zm} t_{0R}. \qquad (37d)$$

Then the angle λ in the post-plastic area is described by:

$$\lambda_{pp} = \lambda(\vartheta) \cong \lambda_0 - \omega_{cpp}(t - t_k) = \lambda_0 - \frac{\omega_{cpp}}{\omega_{zm}}(\vartheta - \vartheta_k). \qquad (38)$$

However the angle ϑ measured and determined from eq. (35) for an chosen position (e.g. $\vartheta = \vartheta(t_0)$ in Fig. 7e) including the elasto-plastic area is given by the formula:

$$\vartheta(t) = \int_{t_0}^{t_k} \omega_{zep}\,dt + \int_{t_k}^{t} \omega_{zpp}\,dt = \vartheta(t_k) - \vartheta(t_o) +$$

$$+ \frac{\upsilon_s}{r_k \omega_{cpp}} \{\cos[\lambda_0 - \Delta\lambda_k - \omega_{cpp}(t - t_k)] - \cos(\lambda_0 - \Delta\lambda_k)\} \tag{38a}$$

After consideration of the eq. (35a) one receives the ϑ value as the function of the trajectory length s:

$$\vartheta(s) = \frac{\omega_{zep}}{\upsilon_s}[s_k(t_k) - s_0(t_0)] + \frac{\upsilon_s}{r_k \omega_{cpp}} \{\cos[\lambda_0 - \Delta\lambda_k -$$

$$- \frac{\omega_{cpp}}{\upsilon_s}(s - s_k(t_k))] - \cos(\lambda_0 - \Delta\lambda_k)]\} \tag{38b}$$

Additionally, some aspects of clod bending and twisting should be considered here. Practically, the clod possesses bigger rotation ω_{cpp} than it had been received at the end of the plastic area. Then the effect of clod bending is stronger, therefore, the clod can even drop down if soil is dry, sandy and plowed at a low speed. For that reason it is reasonable to introduce some additional coefficient exposing the intensity of clod bending upon the moldboard. Any relation can e.g. have the form of bellows and for the new coefficient previously denoted ω_c (see eq. (28)):

$$\omega_{cpp} = \frac{\Delta\lambda_{pp}}{\Delta t_{pp}} \cong \kappa_{pp}\omega_c\,. \tag{39}$$

The coefficient κ_{pp} represents certain average value and it is always bigger than 1; usually 1.5 up to 2.5 or more (dry sand). The clod in that area is again in the elastic state (lesser tension) and behaves in such a way that its shape is going up monotonously to the end of the moldboard surface and than drops down to the furrow. After that moment the problem is left unconsidered. The next problem of our consideration is the trajectory line of the clod's motion.

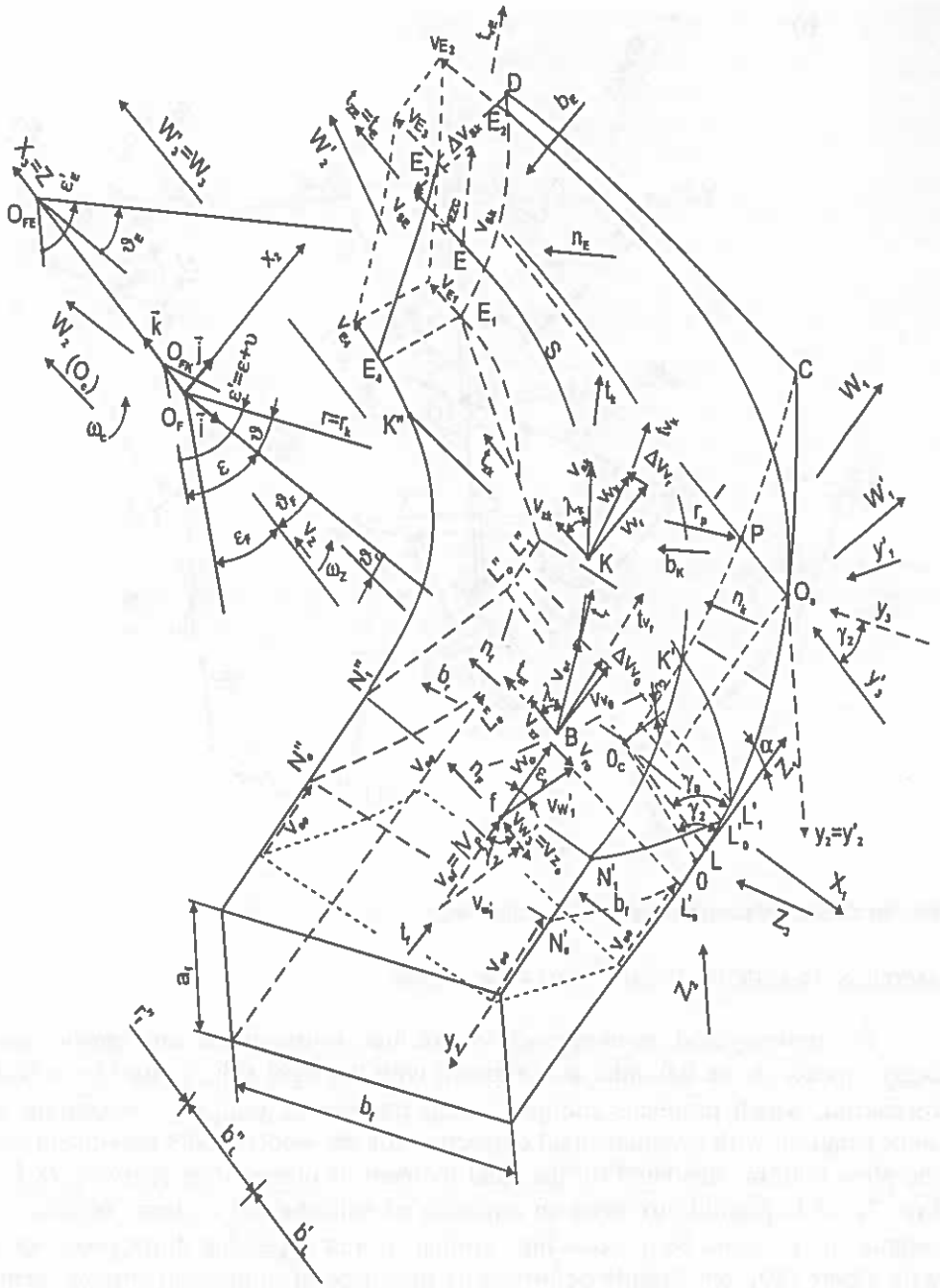

Fig. 8a. Clod motion over plow bottom.

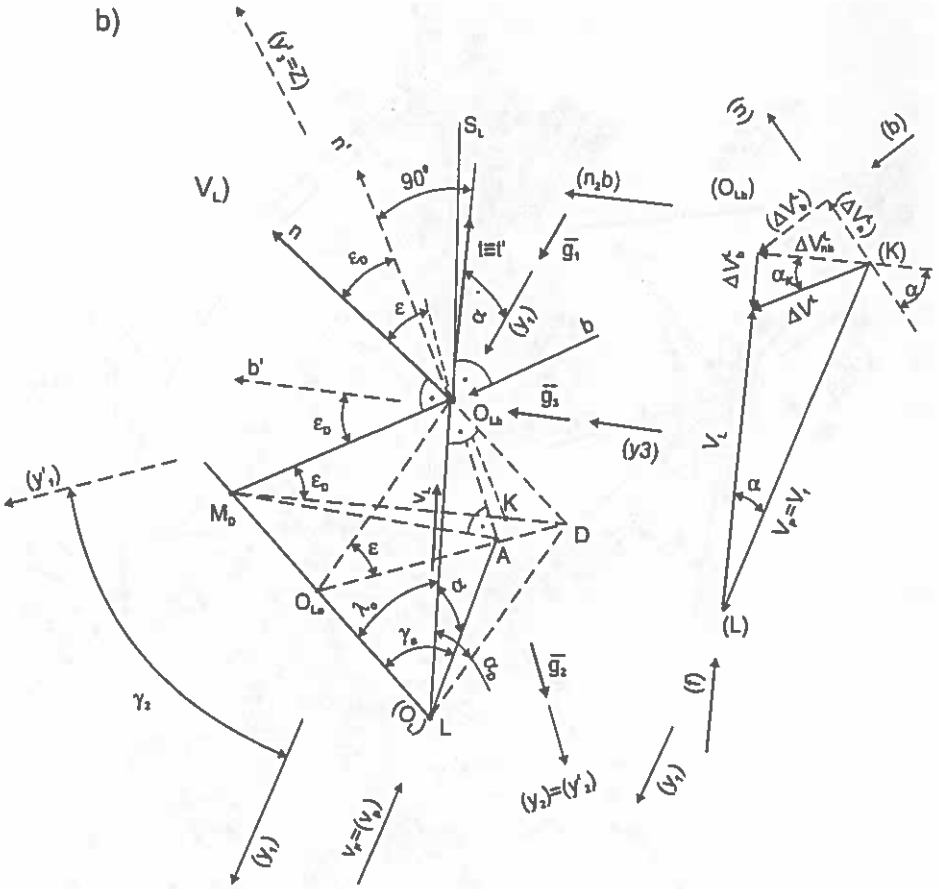

Fig. 8b. Change of particle velocity on the share edge.

MOTION TRAJECTORY OF CLOD PARTICLES

The moving clod, as mentioned before, has, in the elastic and plastic areas, bigger speed on the left side, as compared with the right side, caused by soil deformation, which produces additional clod rotation ω_c (eq.(28)). Assuming the same rotation, with eventual small correction for the whole clod's movement over the plow bottom calculated for the final moment of plastic state (curve $L_l D_L J$ in Fig. 7g) it is possible to write an equation of soil particle motion. Without the rotation ω_c it would be a screw line, similar to that appearing during soil boring with a bore [40], but slightly deformed by the shape of implement surface, generally being not cylindrical.

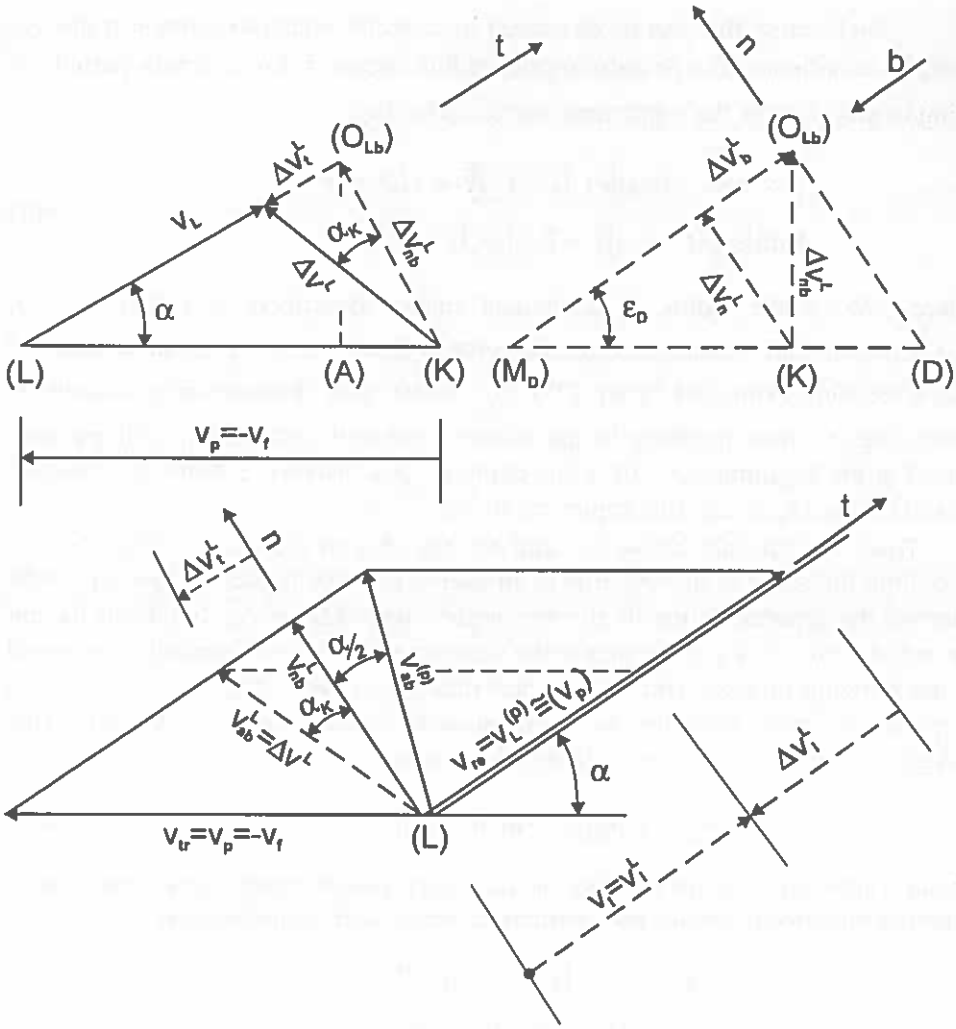

$$\overrightarrow{\Delta V^L}=\overrightarrow{\Delta V_n^L}+\overrightarrow{\Delta V_b^L}+\overrightarrow{\Delta V_t}=\overrightarrow{v_l}-\overrightarrow{v_f}$$

$$\Delta V_{nb}^L \cong v_f \cdot \sin\alpha$$

$$\Delta V_t^L = v_f \cdot \cos\alpha - v_L = \Delta V_{nb}^L \cdot \mathrm{tg}\,\alpha_K$$

$$\Delta V_n^L = \Delta V_{nb}^L \cdot \cos\varepsilon_D$$

$$\Delta V_b^L = \Delta V_{nb}^L \cdot \sin\varepsilon_D$$

$$LO_{Lb}=1$$

$$\mathrm{tg}\,\alpha_D = \sin\lambda_o \mathrm{tg}\,\varepsilon$$

$$\mathrm{tg}\,\varepsilon_D = \cos\lambda_o \mathrm{tg}\,\varepsilon$$

Fig. 8c. Velocity calculation.

Such screw line can be described by a vector equation written in the cylindrical coordinates $O_F r \vartheta z$ defining the radius vector $\vec{r}_p$ for a certain particle P being in motion over the implement surface (Fig. 1a):

$$\begin{aligned}\vec{r}_p &= r(\vartheta, z)\cos[\omega_z(t-t_o)]\vec{i} + r(\vartheta, z)\times \\ &\times \sin[\omega_z(t-t_o)]\vec{j} + b_{s_w}[\omega_z(t-t_o)]\vec{k}\end{aligned} \tag{40}$$

where $r(\vartheta z)$ is the radius of implement surface described by eq.(6) or (6a), $\vec{i}, \vec{j}, \vec{k}$ denote unit vectors for Cartesian system $O_F x_1 x_2 x_3$, ω_z - angular velocity of clod's element, expressed by eq. (27), b_{s_w} - coefficient characterizing a stroke of screw line, t - time referring to the events combined with certain soil particle, placed at the beginning ($t = 0$) at the depth a_f at a distance z_0 from the directrix plane $O_L C D_F$, (t_o is lag-time expressed by eq. (33)).

Thus, the formula above is valid for the chosen particle P_k (Fig. 2a) approaching the share at the lag-time t_0. In such a case the trajectory line (s) would intersect the generating line (l) at some angle λ (eq. (32)) or λ_{pp} (eq. (38)) having the initial value λ_0 (eq. (29)) just at the moment when the soil particle is engaged in the plowing process. But due to clod rotation ω_c (eq. (28)), the angle λ still decreases its value according to the mentioned formula (eq. (32) or (38)). This fact causes that the b_{s_w} factor is changed into a new one:

$$b_{s_n} = r\,\mathrm{ctg}[\lambda_o - \omega_c(t-t_o)] \tag{41}$$

giving a new equation of the motion trajectory (degenerated screw line) traced upon the implement surface and written in vector form as follows [41]:

$$\begin{aligned}\vec{r}_p &= r\cos[\omega_z(t-t_o)]\vec{i} + r\sin[\omega_z(t-t_o)]\vec{j} + \\ &+ r\,\mathrm{ctg}[\lambda_o - \omega_c(t-t_o)]\omega_z(t-t_o)\vec{k}\end{aligned} \tag{42}$$

where $r = r(\vartheta, z)$. That equation can also written in components. Using the system of Cartesian coordinates $O_F x_1 x_2 x_3$ one obtains the components of the radius vector of trajectory line:

$$\begin{aligned}x_1 &= r\cos\omega_z(t-t_o), \\ x_2 &= r\sin\omega_z(t-t_o), \\ x_3 &= r\,\mathrm{ctg}[\lambda_o - \omega_c(t-t_o)]\omega_z(t-t_o) = \upsilon_s\cos[\lambda_o - \omega_c(t-t_o)](t-t_o),\end{aligned} \tag{43}$$

where

$$\omega_z\left(t-t_o\right)=\vartheta-\vartheta_o \tag{43a}$$

is an angle presented with details in Fig. 7g (eq. (34a)) and

$$r\,\omega_{zt}=\upsilon_{\vartheta t}=\upsilon_s\sin\lambda_t. \tag{43b}$$

The Cartesian components above can be transformed into another system of coordinates depending on the needs as they appear. Those equations are in force for a chosen clod's particle (e.g. *P*, Fig. 1a) adjacent to the implement surface during motion. For any other particle (e.g. *R* - Fig. 7g), removed at the beginning for some distance a_R from the furrow's bottom (implement surface), a similar formula is in force, but the radius *r* ought to be replaced by another one: $r_R = r - a_R$. The value for b_{sn} (eq. (41)) should also be sometimes corrected due to abrupt „climbing" of particles caused by clod deformation (swelling).

Additional specific features concerning the plowing problem are not discussed here. Making the use of the equation (43) it is possible to find the components of the velocity, acceleration and then the inertial forces acting upon certain clod particles having certain mass. For that purpose it is convenient to introduce a natural system of coordinates (ξ,η,ζ) adjusted to the trajectory line *s* (Fig. 8) for any point having three unit vectors: normal - *n*, tangent - *t*, binormal - *b*, [20, 30], moving with the point being considered. In that case the vectors of particle speed and acceleration lay down in the osculating plane, traced by tangent and main normal, and at the same time being perpendicular to the binormal of the system being discussed.

In such system of coordinates, the speed change defined by acceleration (a) and time (Δt):

$$\Delta\upsilon = a\Delta t \tag{43c}$$

can be decomposed into two components. One of them is complied with tangent line but another one is perpendicular to the previous one. On that base one can receive a formula for the tangent acceleration of soil particle [20, 30]:

$$a_t=\frac{d\upsilon}{dt} \tag{44}$$

and for the normal acceleration:

$$a_n=\frac{\upsilon^2}{\rho}, \tag{44a}$$

where $\upsilon = \upsilon_s$ (eq. (26)) is the speed of soil particle, ρ - radius of trajectory curving point at a certain point to be defined further. A geometrical sum gives the resultant acceleration:

$$a = \sqrt{a_t^{\,2} + a_n^{\,2}} \,. \tag{45}$$

According to our previous assumption, the speed υ, behind the surface $L_1'K'$ $K''L_1''$ (Fig.1a), has an inclination angle γ (eq. (32)) and the clod is in constant rotation ω_c (eq. (28)) along the trajectory length l_{pp} (Fig.7e). It also has a constant speed $\upsilon = \upsilon_{pp}$ calculated on the base of eq. (25) where, for the value ϑ the corresponding value ϑ_{pm}, suitable to the length

$$l_{pm} \approx r_m \vartheta_{pm} \approx a_f \tag{45a}$$

(depth of plowing), ought to be introduced:

$$\upsilon_{pp} = \upsilon_p \sqrt{\cos^2 \gamma_2 + \left(\sin \gamma_2 - \frac{\xi_1 r_m \upsilon_{pm}}{\upsilon_p} \right)^2} \tag{46}$$

where r_m is the mean radius of clod's cross-section (cf. eq (26)).

Thus the tangent acceleration, within the trajectory length l_{pp} is equal to zero ($a_t = 0$), and therefore the normal acceleration $a_n = a$. For another value of the radius r a proper value of the length of the plastic area ought to be introduced. It should be noted that the influence of some alternation for the resultants of the radius describing the implement surface ($r = r_3 + \Delta r_3'$ see Fig. 3), has not been taken into account here. The only assumption made was $r \cong r_2$ receiving a lot of simplification and not spoiling the results of calculation to much. In a case of some broken bottom (screw-shaped) for tough soil where complete clod's turning is desired, the implement radius alternation ought to be taken into account. The speed υ_{pp} obtained here can be accepted as a medium speed for the entire length of the trajectory starting from the beginning (B_1 in Fig. 7g) up to the end (point E, Fig. 8), simplifying the calculation problem:

$$l_{m0E} = l_m \cong \frac{1}{2} l_c + l_{pm} + l_{pp} \,. \tag{47}$$

To make the formula (44a) most useful, the radius ρ of trajectory curvature should be calculated applying the following procedure. Let us introduce a new parameter u (eq. (37)) and the factor b_{sn} (eq. (41) to the eq. (42). Then the motion trajectory for the particles moving over the implement takes the form:

$$\vec{r}_p = r\cos u\vec{i} + r\sin u\vec{j} + b_{sn}u\vec{k} \tag{48}$$

where: $r = r(\vartheta,z)$ is described by eq. (6) or (6a), but here, for simplicity, is treated as being constant. The length of such curve is calculated after respecting x_3 (eq. (43)) is expressed by [18,47]:

$$s = \int_0^u \left|\frac{d\vec{r}_p}{du}\right| du = \int_0^u \sqrt{r^2 + b_{sn}^2}\, du \tag{49}$$

Introducing relation for u (eq. (37) and relation for ω_c (eq. (28)) in the following form:

$$\omega_c = \frac{\varphi_{\omega c} - \varphi_{\omega c}^0}{t - t_0} \cong \frac{\lambda - \lambda_0}{t - t_0}, \tag{49a}$$

where $\varphi_{\omega_c}, \varphi_{\omega_c}^0$ denote angles related with the rotation ω_c and assumed to be constant. Combining the time $(t - t_0)$ with eq. (43) we can get:

$$x_3 = z = r\,\mathrm{ctg}[\lambda_0 - (\varphi_{\omega_c} - \varphi_{\omega_c}^0)](\vartheta - \vartheta_0) \tag{49b}$$

Inserting of the factor b_{sn} into eq. (49) gives after integration:

$$s(u) = r\sqrt{1 + \mathrm{ctg}^2[\lambda_0 - (\varphi_{\omega_c} - \varphi_{\omega_c}^0)]}\; u = \frac{ru}{\sin[\lambda_0 - (\varphi_{\omega_c} - \varphi_{\omega_c}^0)]} \tag{49c}$$

Combination of eqs (270 and (49a) gives:

$$\vartheta - \vartheta_0 = \frac{\omega_z}{\omega_c}(\varphi_{\omega_c} - \varphi_{\omega_c}^0) \tag{50}$$

Replacing the parameter u in eq. (48) by the length s one ought to use the following relation:

$$u_s = u = \vartheta - \vartheta_0 \cong \frac{s}{s(u_E)} = C_u s, \tag{50a}$$

where

$$C_u = 1/s(u_E) \tag{50b}$$

is the coefficient whereas the inversion of the length $s(u_E)$ corresponds to the last point of the curve considered for the parameter u_E and the angle ϑ corresponds to $\vartheta(s)$, (eq.38b).The trajectory equation related to its length is:

$$\vec{r}_p = r\cos c_u s\vec{i} + r\sin c_u s\vec{j} + b_{sn} c_u s\vec{k}\,, \tag{51}$$

where b_{sn} (eq. (41) is now:

$$b_{sn} = b_{sn}(s) = r\,\mathrm{ctg}[\lambda_0 - (\varphi_{\omega_C} - \varphi^0_{\omega_c})]\,. \tag{51a}$$

Introduction of the coefficient $1/s(u_E)$ into the last equation gives:

$$\vec{r}_p = r\cos\frac{s}{s_{0E}}\vec{i} + r\sin\frac{s}{s_{0E}}\vec{j} + b_{sn}\frac{s}{s_{0E}}\vec{k}\,, \tag{52}$$

where $s_{0E} = s(u_E)$ denotes the entire trajectory length.

Any position of the chosen point passing through the centers of the clod cross section can be obtained from the formula:

$$s(t - t_0) = \upsilon_s(t - t_0), \tag{53}$$

where υ_s is satisfactory defined by eqs (26) or (46), t is the time of the process duration and t_0 is the lag-time (eq. (33)). Any speed of other clod's point R (Fig. 7g) can be estimated using the formula:

$$\upsilon_{sR} = \kappa_\upsilon \upsilon_s z_0 \frac{r - (a_f - a_r)}{r} \tag{53a}$$

where $\upsilon_s(z_0)$ denotes the speed of the soil particle being at the distance z_0 from the directrix plane, κ is a coefficient usually close to 1 whereas a_f , a_R are shown in Fig. 2a.

Similar problem concerns the change of speed of the clods particles caused by the clod's rotation ω_c (eq. (28)). Using the coefficient κ_{pp} (eq. (39)) and neglecting clod's destruction some new relations can be obtained. From

$$\Delta b_L^{\cdot} = \Delta b_l^{\cdot\cdot} \cong 0 \tag{53b}$$

it follows:

$$b_c \cong b_L^{\cdot} + b_L^{\cdot\cdot} \tag{53c}$$

(Fig. 1a), as well as from

$$z_0 = b_L^{\cdot} - z_L^{\cdot} \tag{53d}$$

one obtains

$$R_c \cong r_c + b_L^{"} + z_0 . \tag{53e}$$

Then one can write the relation for the change of the speed caused by the rotation ω_c producing the higher soil deformation at the right side of the clod as compared to the left one:

$$\upsilon_s(z_0) \cong \kappa_{pp}\upsilon_c' \frac{R_c}{r_c + b_c}\sin\lambda_0 , \tag{53f}$$

where υ_c' calculated from the equation (26) is used in the equation (28) whereas r_c, b_c, z_0' are presented in Fig. 1a.

These formulas are sufficient for the first approximation of values. For example in the case of data similar as before (Figs 6b, 4b and 8):

$$\begin{aligned} &l_e = 0.054m, \quad r_s = 0.28m, \quad \upsilon_s = 1.25m/s \quad \omega_z = \omega_{zm} = 3.15s^{-1}, \\ &\omega_c = 0.28s^{-1}, \quad \lambda_o = 42^o, \quad b_f = 0.3m, \quad \kappa_\omega = \frac{0.28}{3.15} \end{aligned} \tag{53g}$$

Place of the start of the process is:

$$\vartheta_o \cong -\left(\vartheta_B + \frac{1}{2}\frac{l_e}{r_s}\right) \cong -\left(15^o + \frac{1}{2}\frac{0.054}{0.028}\cdot\frac{180^o}{\pi}\right) \cong 19^0 \tag{53h}$$

(see Fig. 7e), with the rate: $\dot{\varepsilon}_1 = \dot{\varepsilon}_{w_1}^{I,i} = 2.48$ 1/s (compare Fig. 6b) in a point which is presented in details in a sequence of graphs (cf. Fig. 4b and Fig. 8):

$$\vartheta = \vartheta_E \cong \vartheta_E - arc\sin\frac{b_f}{2r} = 60^o - arc\sin 0.54 = 60^o - 33^o = 27^o, \quad \vartheta_f = 60^o$$

and $\lambda_E = 0$. (see Fig. 4b). The parameter u is equal: $u_{0E} = 27^0 + 19^0 = 0.8$ rd. Thus, the trajectory length (measured in the center of clod cross-section) is:

$$s_{fE} = \frac{3.15}{0.28}\left\{\frac{\cos^2 36^o}{2}\sqrt{1-\cos^4 36^o} + \frac{1}{2}arc\sin\cos^2 36^o\right\} = 1.56m . \tag{53i}$$

In order to study the problem of clod flow over the plow board more precisely, it is necessary to know some feature of motion trajectory of soil particles. It is possible to do so by applying for those purposes certain Frenet's formulas [7, 18, 47]. The first unit vector defining the curve in a space is the tangent unit vector:

$$\bar{t} = \frac{d\bar{r}_p}{ds} = \frac{d\bar{r}_p}{du} \cdot \frac{du}{dt} \cong \frac{\bar{r}'_p}{\sqrt{\bar{r}_p \cdot \bar{r}_p}}, \tag{54}$$

where r_p denotes the radius vector (eqs (40, 42)),

$$r'_p = \frac{d\bar{r}_p}{du}, \tag{54a}$$

u is the parameter (eq. (37)) and s – the length of the curve. The second unit vector is a normal vector defining any curve flexion:

$$\frac{1}{\rho^2} = \frac{d\bar{t}}{ds} \cdot \frac{d\bar{t}}{ds} = \frac{d^2\bar{r}_p}{ds^2} \cdot \frac{d^2\bar{r}_p}{ds^2} = \frac{r^2}{\left(r^2 + b^2_{sn}\right)^2}, \tag{54b}$$

where: ρ is the first radius of curvature, b_{sn} (eq. (41)) denotes a changing factor and r is the radius defined by eqs (6) or (6a). Here the relation:

$$\rho \frac{d^2\bar{r}_p}{ds^2} = \rho \frac{d\bar{t}}{ds} = \bar{n} = \frac{d\bar{t}}{ds} \Big/ \left|\frac{d\bar{t}}{ds}\right| \tag{54c}$$

represents the unit normal vector. The third unit vector discussed here is the binormal unit vector defined as a vector product of two previous ones:

$$\bar{b} = \bar{t} \times \bar{n} = \rho \frac{d\bar{r}_p}{ds} \times \frac{d^2\bar{r}_p}{ds^2} \tag{54d}$$

A relation for the second curvature, i.e. the torsion of the curve is defined by the following mixed vector product:

$$\frac{1}{\tau} = \rho^2 \left[\frac{d\bar{r}_p}{ds}, \frac{d^2\bar{r}_p}{ds^2}, \frac{d^3\bar{r}_p}{ds^3}\right] = -\rho \frac{d^2\bar{r}_p}{ds^2} \cdot \frac{d}{ds}\left[\rho \frac{d\bar{r}_p}{ds} \times \frac{d^2\bar{r}_p}{ds^2}\right] = -\bar{n} \frac{d\bar{b}}{ds} \tag{55}$$

For our trajectory line it equals, at a certain point:

$$\frac{1}{\tau} \cong \frac{b_{sn}}{r^2 + b^2_{sn}} \tag{55a}$$

where τ stands for the second radius of curvature. The third curvature is defined by the Lancret's formula:

$$\frac{1}{k^2} = \frac{1}{\rho^2} + \frac{1}{\tau^2} = \left(\frac{d\vec{n}}{ds}\right)^2 \tag{55b}$$

For another soil particle, removed from the implement surface for a distance a_R (Fig. 7e), another value, adequate for the point being considered, should be given taking also into account some distance z_a from the directive plane defining the lag-time t_{OR} (eq. 34b). Using the above formulas together with the equation (52) and neglecting 2-nd derivative

$$\frac{d^2 b_{sn}}{ds^2} \tag{55c}$$

we can change the formula (54) for the unit tangent vector in the Cartesian coordinates system $O_p x_1 x_2 x_3$ with the unit vectors i,j,k (Fig. 8) into the form:

$$\vec{t} = -\frac{r}{s_{0E}} \sin\frac{s}{s_{0E}} \vec{i} + \frac{r}{s_{0E}} \cos\frac{s}{s_{0E}} \vec{j} + [b_{sn} \frac{1}{s_{0E}} \frac{db_{sn}}{ds} \frac{s}{s_{0E}}]\vec{k} \,. \tag{56}$$

We can calculate the scalar product $\frac{d\vec{t}}{ds}\frac{d\vec{t}}{ds}$ introducing $\frac{d\vec{t}}{ds}$ to the formula (54b) then after transformation and simplification eq. (54c) reads:

$$\vec{n} = \frac{1}{\sqrt{\frac{r^2}{s_{0E}} + 4\left(\frac{db_{sn}}{ds}\right)^2}} \{\frac{-r}{s_{0E}} \cos\frac{s}{s_{0E}} \vec{i} - \frac{r}{s_{0E}} \sin\frac{s}{s_{0E}} \vec{j} + 2\frac{db_{sn}}{ds}\vec{k}\} \tag{57}$$

Putting the time interval t - t_0 from (53) into (41) and replacing ω_c by ω_{cpp} one obtains a new dependence:

$$b_{sn} = r\,\mathrm{ctg}(\lambda_0 - \omega_{cpp}\frac{s}{\upsilon_s}), \tag{58}$$

where the value:

$$\lambda(s) = \lambda_0 - \omega_{cpp}\frac{s}{\upsilon_s} \tag{58a}$$

stands for the previous λ_{pp} (eq. (38)). The factor b_{sn} and its derivative $(\frac{db_{sn}}{ds})$ should be inserted into eqs (56) and (57) giving new formula for the unit vector b:

$$\vec{b} = \vec{t} \times \vec{n} = \frac{r/s_{0E}}{\sqrt{\frac{r^2}{s_{0E}^2} + 4(\frac{db_{sn}}{ds})^2}} \{[2\frac{db_{sn}}{ds}\cos\frac{s}{s_{0E}} + (\frac{b_{sn}}{s_{0E}} + \frac{s}{s_{0E}}\frac{db_{sn}}{ds}) \times$$
$$\times \sin\frac{s}{s_{0E}}]\vec{i} + [2\frac{db_{sn}}{ds}\sin\frac{s}{s_{0E}} - (\frac{b_{sn}}{s_{0E}} + \frac{s}{s_{0E}}\frac{db_{sn}}{ds})\cos\frac{s}{s_{0E}}]\vec{j} + \frac{r}{s_{0E}}\vec{k} \qquad (59)$$

These formulas allow to calculate some values related with clod points being considered here. The calculation results are presented beneath. Putting $\kappa_{pp} = 2$ one obtains $\omega_{cpp} = 0.56\ s^{-1}$ and other data related to the clod's central line passing through the point B_o (replaced by point B_1 (Fig. 7e) for $z_0 = 0$. The results for the beginning point (initiation of process) after some approximations can easily be calculated as follows:

$$a_r \cong \frac{1}{2}a_f = 0.1\,m,\ l_R \cong \frac{1}{2}(a_f + \Delta a_c) = 0.12\ \text{m} \qquad (59a)$$

(estimating $\Delta a_c \cong 0.04$ m (eq. (24d)), $t_{0R} = t_{0B} = 0.044$ s (relatively to the point O_L, (eq. (33b)), $\lambda_0 = 42^0$, $b_{SB1} = 0.292$ m, $\rho_{B1} = 0.502$ m (eq. 54a), $\tau_{B1} = 0.561$ m (eq. 55a).Similar data for the end of the elasto-plastic area (point B_k) take the values: the time of the particle presence in this area (respecting eqs (27) and (32)) is: $t_{epk} = t_{ep} - t_{0B1} = 0.20$s, $\lambda_{Bk} = 35.57^0$, $b_{snBk} = 0.391$ m, $\rho_{Bk} = 0.826$ m, $\tau_{Bk} = 0.591$ m. Finally the data for the end of the process (point E Fig. 8) can be presented in the following way:

$$s_{0E} = 0.36m,\quad (eq.\ (49a)),\quad t_{0E} = 0.288s,\quad (eq.\ (53)),$$
$$\lambda_E = 32.37^0,\ b_{snE} = 0.442\ m,\ \rho_E = 0.978m,\quad \tau_E = 0.619m \qquad (59b)$$

The normal acceleration (a_n, eq. (44)) has for certain points the following values: in the point of the beginning (point B_1) when

$$\upsilon_0 = \upsilon_{B_1} \cong \upsilon_p = 1.4\,\frac{m}{s},\quad a_{nB_1} = 3.31\,\frac{m}{s^2}, \qquad (59c)$$

in the point B_k (when $\upsilon_s = 1.25$ m/s) $a_{nBk} = 1.98$ m/s^2, and finally at the end (point E, $\upsilon_{sE} = \upsilon_s$) $a_{nE} = 1.60$ m/s^2. This acceleration creates some inertial forces dependent on masses involved in the motion, which will be studied in the next paper dealing with the dynamic effects and volume deformation of plowed soil.

REFERENCES

1. **Appazov R.F., Sytin O.G.:** Design methods for trajectories of carrier rockets and satellites (in Russian), „Nauka", Moscow, 1987.
2. **Bernacki H., Haman J., Kanafojski C.:** Theory and construction of agricultural machinery, Central Institute of Scientific, Technical and Economical Information, Warsaw, 1972.
3. **Borodachev J. P.:** Guidebook for constructors of road machines (in Russian), Mashinostroenie, Moscow, 1973.
4. **Bronstein J.N., Semiendiayev K.A.:** Mathematics (in Russian), „Nauka", Moscow, 1967.
5. **Bronstein J.N., Semiendiayev K.A.:** Handbook of mathematics for engineers (in Polish), PWN, Warsaw, 1998.
6. **Cytovich N.A.:** Soil mechanics (in Russian), GILSA, Moscow 1951.
7. **Duschek A., Hochreiner A.:** Tensorrechnung in analitischer Darstellung, III Teil, Wien, Springer-Verlag 1955.
8. **Erbel S., Kaczyński K.:** Theory of plasticity (in Polish), PWN, Warsaw 1973.
9. **Galwitz K., Szwaj S.:** Ein Kraftmessgerat mit Kardanwelle, Grundlagen der Landtechnik 3, 23-46, 1973.
10. **Gill W.R., Van den Berg G.E.:** Soil dynamics in tillage and traction, U.S. Department of Agriculture, Washington, 1967.
11. **Gologurski T.M.:** Work of machinery in earth (in Polish), TPPNR, Kraków, 1911.
12. **Goriachkin V. P.:** Theory of plow (in Russian), Moscow, 1927.
13. **Griffith D.V.:** Failure criteria interpretation based on Mohr-Coulomb friction, Jour. Geotech. Eng., 12, 151-175, 1988.
14. **Haman J.:** Study of two cases of selfexcited vibrations of plow bottom (in Polish), Annales UMCS, sec. E, 14, 19-36, 1961.
15. **Hill R.:** Mathematical theory of plasticity, Oxford Press, 1950.
16. **Hoffman O., Sachs G.:** Introduction to theory of plasticity for engineers, Mac Graw-Hill, 1953.
17. **Joselin de Jong G.:** Statics and kinematics of plastic deformation of granular media (in Polish), Ossolineum, Wrocław, 1965.
18. **Karaśkiewicz E.:** Basic theory of vectors and tensors (in Polish), PWN, Warsaw, 1975.
19. **Kisiel I., Dmitruk S., Lysik B.:** Bases of Soil Rheology (in Polish), Arkady, Warsaw, 1969.
20. **Konarzewski Z.:** Mechanics and strength of materials (in Polish), WNT, Warsaw, 1974.
21. **Kunstetter S.:** Bases of construction of machines (in Polish), WNT, Warsaw, 1980.
22. **Leyko J.:** Bases of mechanics (in Polish), PWN, Warsaw, 1978.
23. **Nowacki W.:** Theory of micropolar elasticity (in Polish), PWN, Warsaw, 1979.
24. **O'Calahan J.H.:** The handling of soil by moldboard plows, Journ. of Agric. Eng. Res., 10, 345-361, 1965.
25. **Olszak. W., Perzyna P., Sawczuk A.:** Theory of plasticity (in Polish), PWN, Warsaw, 1965.
26. **Piętkowski R., Czarnota – Bojarski R.:** Soil mechanics (in Polish), Arkady, Warsaw, 1964
27. **Pukos A., Walczak R.:** Theoretical foundation of soil mechanical properties (in Polish), Problemy Agrofizyki, 7, 1973.
28. **Pukos A.:** On the applicability of visco-elastic models in soil mechanics, Proc. IInd International Conference on Agricultural Materials, 24-30 August, Agricultural University, Godollo, Hungary, 1980.
29. **Pukos A.:** Soil compaction and pore size distribution (in Polish), Problemy Agrofizyki, Ossolineum, Wrocław, 61, 1990.
30. **Skalmierski B.:** Mechanics (in Polish), PWN, Warsaw, 1977.
31. **Sobotka Z.:** Conditions of plasticity and limit states, Ossolineum, Wrocław, 1966.
32. **Smirnov W.I.:** Contemporary mathematics (in Polish), PWN, Warsaw, 1958.

33. **Soene W.:** Anpassung der Pflugkorperform an Fahrgeschwindigkeiten, Grundlagen der Landtechnik, 12, 67-91, 1960.
34. **Sokolnikov J.S.:** Tensor analysis, John Willey and Sons, New York. 1958.
35. **Sokolowski W.W.:** Statics of granular media (in Polish), PWN, Warsaw, 1958.
36. **Szwaj S.:** Basic investigations on soil mechanics in application to the farm machinery design (in Polish), Roczn. Nauk Roln., C-1, 68, 1966.
37. **Szwaj S.:** Three selected papers from Arch. Bud. Masz: Shearing strength of soil during quick deformation (vol. 11, No. 3, 1965), Quick compression of soil in triaxial test device (vol. 12, No. 1, 1966), Quick strain processes in soil (vol. 15, No. 1, 1968 (in Polish), published for the US Dept. Of Agriculture by the National Center for Scientific, Technical and Economical Information, Warsaw, 1974.
38. **Szwaj S.:** Memory effect in soil subjected to rapid loading in triaxial apparatus, Proc. IIIrd European Conference ISTVS, September, Warsaw, 1986.
39. **Szwaj S.:** Soil treatment with tools of flat work path (in Polish), Roczn. Nauk Roln., ser. D, 171, Warsaw, 1982.
40. **Szwaj S.:** Construction of the hypothesis of drainers motion created with the use of question path method, Archives of Transport, vol. 4 No. 2, 1992.
41. **Szwaj S.:** Tools for flat work path with inclined generating lines, Proc. Ist Int. Conf. ISTVS European Office, 23-24 September, Wroclaw, 1996.
42. **Terzagi K.:** Theoretical Soil Mechanics, John Willey and Sons, New York, 1956.
43. **Trajdos T.:** Mathematics (in Polish), WNT, Warsaw, 1971.
44. **Walczak R.:** Model investigation of water binding energy in soils of different compaction, Zesz. Probl. Post. Nauk Roln., 197, 11-43, 1977.
45. **Wiłun Z.:** Bases of geotechnics (in Polish), PWN, Warsaw, 1982.
46. **Wrona W.:** Mathematics (in Polish), PWN, Warsaw, 1964.
47. **Wu T. H. at al.:** Study of soil-root interaction, Geotech. Eng., 12, 36-51, 1988.
48. **Zielenin A. N.:** Physical basis of soil cutting theory, AN USSR, Moscow, 1950.

PLOWING THEORY

Summary

Plowing is the most complicated and energy consuming tillage process in agricultural soils. One of its main goals is to obtain a soil bulk density optimal for the growth of plants. The plowing problem has been considered theoretically in the present paper and it was assumed that the clod undergoes four loading processes during plowing. Two of them are bending deformations whereas the other two can be represented by rotations. Different moldboard shapes (circle, ellipse, parabola and hyperbola) are assumed and the moldboard shapes together with the plow bottom action, soil mass deformation, clod formation and motion over the moldboard are introduced in the form of the kinetic equations. They can be used for the prediction of dynamical effects and volume changes resulting in the prediction of the final bulk density. Theoretical consideration have been illustrated using figures and experimental data.

Keywords: soil mechanics, soil plowing, soil dynamics, tillage

TEORIA ORKI

Streszczenie

Orka jest najbardziej skomplikowanym i energochłonnym zabiegiem uprawowym w rolnictwie. Jednym z jej głównych celów jest uzyskanie gęstości objętościowej gleby optymalnej dla wzrostu i rozwoju roślin. W pracy rozpatrzono problem orki w sposób teoretyczny i założono, że skiba podlega czterem programom obciążenia w trakcie orki. Dwa z tych obciążeń są odkształceniami polegającymi na zginaniu, a pozostałe dwa mogą być przedstawione jako obroty. Założono różne kształty odkładnic (koło, elipsa, hiperbola i parabola) i przedstawiono równania kinetyki działania pługa, odkształcenia ośrodka glebowego, tworzenia się skiby i jej ruchu po odkładnicy. Mogą one być wykorzystane do przewidywania efektów dynamicznych i zmian objętościowych prowadzących do przewidywania końcowej gęstości objętościowej. Rozważania teoretyczne zostały zilustrowane przy pomocy rysunków i danych eksperymentalnych.

Słowa kluczowe: mechanika gleby, orka, dynamika gleby, uprawa roli.